

Predicting Drug-Gene Relations via Analogy Tasks with Word Embeddings

Hiroaki Yamagiwa^{1,*}, Ryoma Hashimoto^{2,†}, Kiwamu Arakane^{3,◊}, Ken Murakami^{3,◊}, Shou Soeda^{3,◊}, Momose Oyama^{1,4,*}, Mariko Okada^{3,◊}, and Hidetoshi Shimodaira^{1,4,†}

¹Kyoto University

²Recruit Co., Ltd.

³Institute for Protein Research, Osaka University

⁴RIKEN

^{*}{hiroaki.yamagiwa, oyama.momose}@sys.i.kyoto-u.ac.jp,

[†]ryoma.hashimoto@r.recruit.co.jp

[◊]{k.arakane, k-mrkm, shousoeda, mokada}@protein.osaka-u.ac.jp,

[†]shimo@i.kyoto-u.ac.jp

ABSTRACT

Natural language processing (NLP) is utilized in a wide range of fields, where words in text are typically transformed into feature vectors called embeddings. BioConceptVec is a specific example of embeddings tailored for biology, trained on approximately 30 million PubMed abstracts using models such as skip-gram. Generally, word embeddings are known to solve analogy tasks through simple vector arithmetic. For instance, *king – man + woman* predicts *queen*. In this study, we demonstrate that BioConceptVec embeddings, along with our own embeddings trained on PubMed abstracts, contain information about drug-gene relations and can predict target genes from a given drug through analogy computations. We also show that categorizing drugs and genes using biological pathways improves performance. Furthermore, we illustrate that vectors derived from known relations in the past can predict unknown future relations in datasets divided by year.

Introduction

Natural language processing (NLP) is a computer technology for processing human language. NLP is used in various applications, such as machine translation^{1,2}, sentiment analysis^{3,4}, and sentence similarity computation^{5,6}. Many of these applications use models such as skip-gram^{7,8} or BERT⁴ to convert words in text to embeddings or distributed representations, which are feature vectors with hundreds of dimensions. In particular, skip-gram is a method that learns high-performance embeddings by predicting the surrounding words of a word in a sentence. These embeddings form the foundational building blocks of recent advances in large language models, enabling models to understand and generate human language with unprecedented accuracy and coherence.

Mikolov et al.⁷ showed that skip-gram embeddings have properties such as $\mathbf{u}_{\text{king}} - \mathbf{u}_{\text{man}} + \mathbf{u}_{\text{woman}} \approx \mathbf{u}_{\text{queen}}$, where the vector \mathbf{u}_w represents the embedding of word w . In the embedding space, the vector differences such as $\mathbf{u}_{\text{king}} - \mathbf{u}_{\text{man}}$ and $\mathbf{u}_{\text{queen}} - \mathbf{u}_{\text{woman}}$ can be seen as vectors representing the *royalty* relation. Since these relations are not explicitly taught during the training of skip-gram, the embeddings acquire these properties spontaneously. Solving questions such as “If *man* corresponds to *king*, what does *woman* correspond to?” requires understanding the relations between words. This type of problem is known as an *analogy task* and is used to evaluate a model’s language comprehension and reasoning skills. In this example, the model must understand the *royalty* relations from *man* to *king* and apply a similar relation to *woman*. Allen and Hospedales⁹ explained why analogy computation with such simple vector arithmetic can effectively solve analogy tasks.

Recently, NLP methods have also gained attention in the field of biology^{10–12}. However, since traditional skip-gram models are typically trained on web corpora, they do not properly handle the specialized terms that appear in biological texts. In particular, when multiple words represent the same concept, these concepts should be normalized beforehand and represented by the same embedding. With this in mind, Chen et al.¹³ proposed a method to compute word embeddings of biological concepts using approximately 30 million PubMed abstracts in which the mentions of these concepts had been previously normalized using PubTator¹⁴. PubTator is an online tool that supports the automatic annotation of biomedical text and aims at extracting specific information efficiently. Particularly, it can identify the mentions of biological concepts and entities within text and classify them into appropriate categories (e.g., diseases, genes, drugs). They trained four embedding models, including skip-gram, and named their embeddings BioConceptVec, and assessed the usefulness of BioConceptVec in two ways: intrinsic

and extrinsic evaluations. For intrinsic evaluations, they identified related genes based on drug-gene and gene-gene interactions using cosine similarity of the embeddings. For extrinsic evaluations, they performed protein-protein interaction prediction and drug-drug interaction extraction using neural network classifiers with the embeddings. However, the embeddings' performance on solving the analogy tasks is yet to be explored.

In this study, we consider analogy tasks in biology using word embeddings. We trained skip-gram embeddings similarly to BioConceptVec, aiming to compare them with BioConceptVec embeddings and to develop embeddings from datasets divided by year in an extended experiment. To evaluate the performance of analogy computation, we focus on predicting target genes from a given drug. These target genes are associated with proteins that the drug interacts with, and these interactions are called *drug-target interactions* (DTIs)^{15,16}. In this paper, we will refer to these connections as *drug-gene relations*. Our research aims to show that embeddings learned from biological text data contain information about drug-gene relations. In the example of $\mathbf{u}_{\text{king}} - \mathbf{u}_{\text{man}} + \mathbf{u}_{\text{woman}} \approx \mathbf{u}_{\text{queen}}$, the vector differences $\mathbf{u}_{\text{king}} - \mathbf{u}_{\text{man}}$ and $\mathbf{u}_{\text{queen}} - \mathbf{u}_{\text{woman}}$ represent the *royalty* relation. However, there are multiple drug-gene pairs with drug-gene relations, and a single drug often has multiple target genes. Therefore, we calculate the vector differences between the embeddings of each drug and its target genes and average these vector differences to define a mean vector representing the relation.

To evaluate the performance in predicting drug-gene relations, we use data derived from KEGG¹⁷ as the ground truth. We first consider analogy tasks in the global setting where all drugs and genes are included and demonstrate high performance in solving these tasks. Next, to consider more detailed analogy tasks, we use information common to both drugs and genes. Specifically, we focus on biological pathways to categorize drugs and genes. To do this, we use a list of human pathways from the KEGG API. We group all drugs and genes that are associated with the same pathway into a single category and define vectors representing drug-gene relations for each pathway. In this pathway-wise setting, we demonstrate that using these vectors in the analogy computation can improve its performance. Finally, as an application of analogy computation, we investigate the potential of our approach to predict unknown drug-gene relations. For this purpose, we divide the vocabulary by year to distinguish between known and unknown drug-gene relations. We then train skip-gram embeddings using PubMed abstracts published before the specified year and redefine vectors representing the known relations to predict unknown relations. The experimental results show that our approach can predict unknown relations to a certain extent.

The structure of this paper is as follows. First, we explain related work and detail our approach in this study. In the following sections, we perform experiments for each setting and evaluate the performance using metrics such as top-1 accuracy. Finally, we discuss specific prediction results and then conclude.

Related work

Analogy computation of word embeddings trained from corpora in a particular field of natural science can be used to predict the relations that exist between specialized concepts or terms. Tshitoyan et al.¹⁸ have shown that the relation between specialized concepts in the materials science field such as “ferromagnetism – NiFe + IrMn \approx antiferromagnetism” can be correctly predicted using analogy computation of word embeddings trained with domain-specific literature.

In the biomedical field, capturing the relations between biomedical concepts such as drug-drug and protein-protein interaction is an important issue. Word embeddings trained on biomedical domain corpora have been used to predict drug-drug interactions for new drugs¹⁹ and to construct networks of gene-gene interactions²⁰. Also, neural networks have been used in a number of studies to predict these relations^{21–25}.

Technologies developed in NLP, not limited to word embedding, have been applied to a wide variety of problems in the biomedical domain: Müller et al.²⁶ have created an online literature search and curation system using an “ontology dictionary” obtained by text mining, and Friedman et al.²⁷ have used syntactic parsing to extract and structure information about cellular pathways from biological literature. Yeganova et al.²⁸ normalize synonyms in the biomedical literature by word embedding similarity. Furthermore, Du et al.²⁹ applied the word embedding algorithm to gene co-expression across the transcriptome to compute vector representations of genes. In recent years, there has also been intensive research on fine-tuning BERT⁴ and other pre-trained language models to the biomedical domain^{10,30,31}.

Methods

Analogy tasks

This section illustrates a basic analogy task, a problem setting commonly used in benchmark tests to evaluate the performance of word embedding models. We define \mathcal{V} as the vocabulary set, and $\mathbf{u}_w \in \mathbb{R}^K$ as the word embedding of word $w \in \mathcal{V}$. In skip-gram models, the “closeness of word embeddings” measured by cosine similarity correlates well with the “closeness of word meanings”⁷. For example, in word2vec⁷, $\cos(\mathbf{u}_{\text{media}}, \mathbf{u}_{\text{press}}) = 0.601 > \cos(\mathbf{u}_{\text{media}}, \mathbf{u}_{\text{car}}) = 0.020$. This result shows that the embedding of *media* is closer to the embedding of *press* than to the embedding of *car*. This is consistent with the rational human interpretation that *media* is semantically closer to *press* than to *car*. The task for predicting relations between words is



Figure 1. Analogy computations by adding the relation vector. (a) Example of a basic analogy task. The question “If *man* corresponds to *king*, what does *woman* correspond to?” is solved by adding the relation vector $\mathbf{v}_{royalty}$ to \mathbf{u}_{woman} . (b) Example of an analogy task in setting G . The target genes of the drug d are g_1 , g_2 , and g_3 , predicted by adding the relation estimator $\hat{\mathbf{v}}$ to the drug embedding \mathbf{u}_d .

known as an analogy task, and word embeddings can effectively solve analogy tasks using vector arithmetic⁷. For example, to solve the question “If *man* corresponds to *king*, what does *woman* correspond to?”, using pre-trained skip-gram embeddings, we search for $w \in \mathcal{V}$ that maximizes $\cos(\mathbf{u}_{king} - \mathbf{u}_{man} + \mathbf{u}_{woman}, \mathbf{u}_w)$, and find $w = queen$, indicating

$$\mathbf{u}_{king} - \mathbf{u}_{man} + \mathbf{u}_{woman} \approx \mathbf{u}_{queen}. \quad (1)$$

This analogy computation is illustrated in Fig. 1a. Here, the vector $\mathbf{v}_{royalty}$ represents the *royalty* relation between *man* and *king*, and is defined as the vector difference between \mathbf{u}_{king} and \mathbf{u}_{man} :

$$\mathbf{v}_{royalty} := \mathbf{u}_{king} - \mathbf{u}_{man}. \quad (2)$$

Adding the *royalty* relation vector $\mathbf{v}_{royalty}$ to \mathbf{u}_{woman} then yields \mathbf{u}_{queen} :

$$\mathbf{u}_{woman} + \mathbf{v}_{royalty} \approx \mathbf{u}_{queen}. \quad (3)$$

Analogy tasks for drug-gene pairs

In this section, based on the basic analogy task from the previous section, we explain analogy tasks for predicting target genes from a drug. First, we consider the global setting, where all drugs and genes in the vocabulary set are used. Then, we consider the pathway-wise setting, where drugs and genes are categorized based on biological pathways.

Global setting

As a first step, based on the basic analogy task, we consider analogy tasks in the global setting, where all drugs and genes are used. We define $\mathcal{D} \subset \mathcal{V}$ and $\mathcal{G} \subset \mathcal{V}$ as the sets of all drugs and genes, respectively. We also define $\mathcal{R} \subset \mathcal{D} \times \mathcal{G}$ as the set of drug-gene pairs with drug-gene relations. Thus, if a drug $d \in \mathcal{D}$ and a gene $g \in \mathcal{G}$ have a drug-gene relation, the pair (d, g) is in \mathcal{R} . For illustrating the positions of drugs and genes in the 100-dimensional BioConceptVec skip-gram embeddings, we sampled 200 drug-gene pairs in \mathcal{R} and plotted them in Fig. 2a using Principal Component Analysis (PCA). The vector difference between the mean embeddings of drugs and genes points in roughly the same direction as the vector differences between the embeddings of each sampled drug and its target gene.

To apply the analogy computation of Eq. (3) to drug-gene pairs $(d, g) \in \mathcal{R}$, we consider the analogy tasks for predicting the gene g from the drug d . Using the vector \mathbf{v} representing the drug-gene relation, we predict \mathbf{u}_g by adding the relation vector \mathbf{v} to \mathbf{u}_d as follows:

$$\mathbf{u}_d + \mathbf{v} \approx \mathbf{u}_g. \quad (4)$$

Thus, we need methods for estimating the relation vector \mathbf{v} . In Eq. (2), the *royalty* relation vector $\mathbf{v}_{royalty}$ is calculated from the embeddings of the given pair $(man, king)$. Therefore, we estimate the relation vector \mathbf{v} from the embeddings of genes and drugs. The following equation gives the vector difference between the mean vectors of \mathcal{D} and \mathcal{G} as a naive estimator of \mathbf{v} :

$$\hat{\mathbf{v}}_{\text{naive}} := \mathbf{E}_{\mathcal{G}}\{\mathbf{u}_g\} - \mathbf{E}_{\mathcal{D}}\{\mathbf{u}_d\}, \quad (5)$$

$$\mathbf{E}_{\mathcal{D}}\{\mathbf{u}_d\} = \frac{1}{|\mathcal{D}|} \sum_{d \in \mathcal{D}} \mathbf{u}_d, \quad \mathbf{E}_{\mathcal{G}}\{\mathbf{u}_g\} = \frac{1}{|\mathcal{G}|} \sum_{g \in \mathcal{G}} \mathbf{u}_g. \quad (6)$$

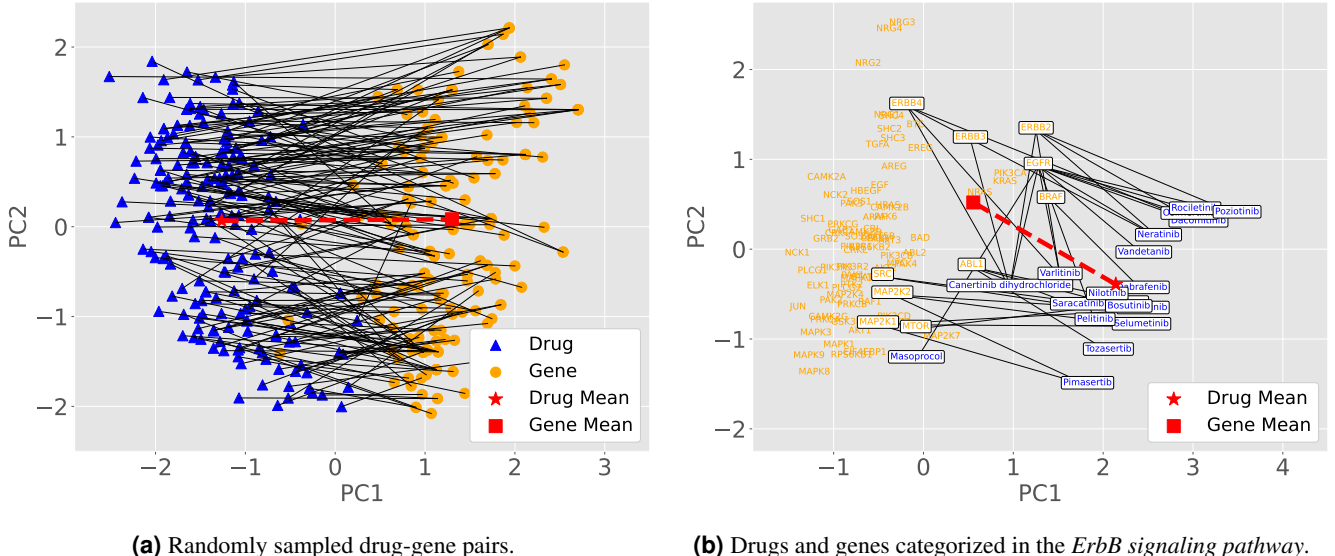


Figure 2. 2-d visualization of embeddings using PCA. Drugs and genes are shown in blue and orange, respectively. Solid lines represent the relations. The symbols \star and \blacksquare represent the mean embeddings of the drugs and genes, respectively. The direction of the dashed line connecting these two symbols can be considered as the drug-gene relation vector. (a) Randomly sampled 200 drug-gene pairs from \mathcal{R} . The mean embeddings are computed by Eq. (9). (b) Drugs $d \in \mathcal{D}_p$ and genes $g \in \mathcal{G}_p$ for $p = \text{ErbB signaling pathway}$. Those that have drug-gene relations are shown in boxes. The mean embeddings are computed by Eq. (16).

In Eq. (6), $E_{\mathcal{D}}\{\cdot\}$ and $E_{\mathcal{G}}\{\cdot\}$ represent the sample means over the set of all drugs \mathcal{D} and the set of all genes \mathcal{G} , respectively. However, the definition of \hat{v}_{naive} in Eq. (5) includes the embeddings of unrelated genes and drugs. Therefore, a better estimator may be defined by using only the pairs $(d, g) \in \mathcal{R}$. We consider the estimator \hat{v} as the mean of the vector differences $\mathbf{u}_g - \mathbf{u}_d$ for $(d, g) \in \mathcal{R}$ as follows:

$$\hat{v} := E_{\mathcal{R}}\{\mathbf{u}_g - \mathbf{u}_d\} = \frac{1}{|\mathcal{R}|} \sum_{(d,g) \in \mathcal{R}} (\mathbf{u}_g - \mathbf{u}_d), \quad (7)$$

where $E_{\mathcal{R}}\{\cdot\}$ is the sample mean over the set of drug-gene pairs \mathcal{R} . For easy comparison with Eq. (5), Eq. (7) is rewritten as the difference of mean vectors:

$$\hat{v} = E_{\mathcal{R}}\{\mathbf{u}_g\} - E_{\mathcal{R}}\{\mathbf{u}_d\}, \quad (8)$$

$$E_{\mathcal{R}}\{\mathbf{u}_g\} = \frac{1}{|\mathcal{R}|} \sum_{(d,g) \in \mathcal{R}} \mathbf{u}_g, \quad E_{\mathcal{R}}\{\mathbf{u}_d\} = \frac{1}{|\mathcal{R}|} \sum_{(d,g) \in \mathcal{R}} \mathbf{u}_d. \quad (9)$$

To measure the performance of the estimator \hat{v} in Eq. (7), we prepare the evaluation of the analogy tasks. We define D and G as the sets of drugs and genes contained in \mathcal{R} , respectively. Specifically, we define $D := \pi_{\mathcal{D}}(\mathcal{R})$ as the set of drugs d such that $(d, g) \in \mathcal{R}$ for some genes g , and $G := \pi_{\mathcal{G}}(\mathcal{R})$ as the set of genes g such that $(d, g) \in \mathcal{R}$ for some drugs d , where the projection operations $\pi_{\mathcal{D}}$ and $\pi_{\mathcal{G}}$ are defined as

$$\pi_{\mathcal{D}} : \mathcal{R} \mapsto \{d \mid (d, g) \in \mathcal{R}\} \subset \mathcal{D}, \quad \pi_{\mathcal{G}} : \mathcal{R} \mapsto \{g \mid (d, g) \in \mathcal{R}\} \subset \mathcal{G}. \quad (10)$$

We also define $[d] \subset \mathcal{G}$ as the set of genes that have drug-gene relations with a drug $d \in D$, and $[g] \subset \mathcal{D}$ as the set of drugs that have drug-gene relations with a gene $g \in G$. These are formally defined as

$$[d] := \{g \mid (d, g) \in \mathcal{R}\} \subset \mathcal{G}, \quad [g] := \{d \mid (d, g) \in \mathcal{R}\} \subset \mathcal{D}. \quad (11)$$

Given the above, we perform the analogy computation in the following setting.

Set	Size	Symbol	Elements of the set
\mathcal{D}_p	19	d	Bosutinib, Canertinib dihydrochloride, Dabrafenib, Dacomitinib, Masoprocol, Neratinib, Nilotinib, Osimertinib, Pelitinib, Pimasertib, Pozotinib, Rociletinib, Saracatinib, Selumetinib, Temsirolimus, Tozasertib, Trametinib, Vandetanib, Varlitinib
\mathcal{G}_p	84	g	ABL1, ABL2, AKT1, AKT2, AKT3, ARAF, AREG, BAD, BRAF, BTC, CAMK2A, CAMK2B, CAMK2D, CAMK2G, CBL, CBLB, CDKN1A, CDKN1B, CRK, CRKL, EGF, EGFR, EIF4EBP1, ELK1, ERBB2, ERBB3, ERBB4, EREG, GAB1, GRB2, GSK3B, HBEGF, HRAS, JUN, KRAS, MAP2K1, MAP2K2, MAP2K4, MAP2K7, MAPK1, MAPK10, MAPK3, MAPK8, MAPK9, MTOR, MYC, NCK1, NCK2, NRAS, NRG1, NRG2, NRG3, NRG4, PAK1, PAK2, PAK3, PAK4, PAK5, PAK6, PIK3CA, PIK3CB, PIK3CD, PIK3R1, PIK3R2, PIK3R3, PLCG1, PLCG2, PRKCA, PRKCB, PRKCG, PTK2, RAF1, RPS6KB1, RPS6KB2, SHC1, SHC2, SHC3, SHC4, SOS1, SOS2, SRC, STAT5A, STAT5B, TGFA
\mathcal{R}_p	34	(d, g)	(Bosutinib, ABL1), (Bosutinib, SRC), (Canertinib dihydrochloride, EGFR), (Canertinib dihydrochloride, ERBB2), (Canertinib dihydrochloride, ERBB3), (Canertinib dihydrochloride, ERBB4), (Dabrafenib, BRAF), (Dacomitinib, EGFR), (Dacomitinib, ERBB2), (Dacomitinib, ERBB4), (Masoprocol, EGFR), (Neratinib, EGFR), (Neratinib, ERBB2), (Neratinib, ERBB4), (Nilotinib, ABL1), (Osimertinib, EGFR), (Pelinib, EGFR), (Pimasertib, MAP2K1), (Pimasertib, MAP2K2), (Pozotinib, EGFR), (Pozotinib, ERBB2), (Rociletinib, EGFR), (Saracatinib, ABL1), (Saracatinib, SRC), (Selumetinib, MAP2K1), (Selumetinib, MAP2K2), (Temsirolimus, MTOR), (Tozasertib, ABL1), (Trametinib, MAP2K1), (Trametinib, MAP2K2), (Vandetanib, EGFR), (Varlitinib, EGFR), (Varlitinib, ERBB2), (Varlitinib, ERBB4)

Table 1. \mathcal{D}_p , \mathcal{G}_p , and \mathcal{R}_p for the pathway p , where p is the *ErbB signaling pathway*. Note that we only use concepts that exist in BioConceptVec and can be converted to names, so they do not exactly match the actual drugs and genes categorized in the biological pathway. In addition, we have changed the notation of some drugs from compounds to more readable names.

Setting G. In the analogy tasks, the set of answer genes for a query drug $d \in D$ is $[d]$. The predicted gene is $\hat{g}_d = \operatorname{argmax}_{g \in \mathcal{G}} \cos(\mathbf{u}_d + \hat{\mathbf{v}}, \mathbf{u}_g)$ and if $\hat{g}_d \in [d]$, then the prediction is considered correct. We define $\hat{g}_d^{(k)}$ as the k -th ranked $g \in \mathcal{G}$ based on $\cos(\mathbf{u}_d + \hat{\mathbf{v}}, \mathbf{u}_g)$. For the top- k accuracy, if any of the top k predictions $\hat{g}_d^{(1)}, \dots, \hat{g}_d^{(k)} \in [d]$, then the prediction is considered correct.

Unlike in the basic analogy task, there may be multiple target genes for a single drug. While the basic analogy task is one-to-one, we address one-to-many analogy tasks in this study, where a single source may correspond to multiple targets³². Analogy computation for setting G is illustrated in Fig. 1b, where the set of answer genes $[d]$ consists of g_1, g_2 , and g_3 . If the predicted gene \hat{g}_d is one of these three genes, then the prediction is considered correct. Note that the analogy tasks for predicting drugs from a query gene can also be defined similarly. See Supplementary Information 1.3 for details.

Pathway-wise setting

As a next step, based on the analogy tasks in setting G, we consider more detailed analogy tasks. To do this, we consider the analogy tasks in the pathway-wise setting, where drugs and genes are categorized using biological pathways. We define \mathcal{P} as the set of pathways p , and $\mathcal{D}_p \subset \mathcal{D}$ and $\mathcal{G}_p \subset \mathcal{G}$ as the sets of drugs and genes categorized in each pathway $p \in \mathcal{P}$, respectively. We then restrict the set \mathcal{R} to each pathway p and define the subset of \mathcal{R} as:

$$\mathcal{R}_p := \{(d, g) \in \mathcal{R} \mid d \in \mathcal{D}_p, g \in \mathcal{G}_p\} \subset \mathcal{D}_p \times \mathcal{G}_p. \quad (12)$$

A specific example of these sets for the *ErbB signaling pathway* is shown in Table 1, and their BioConceptVec skip-gram embeddings are illustrated in Fig. 2b. The vector difference between the mean embeddings of drugs and genes roughly points in the same direction as the vector differences between the embeddings of each drug and its target gene in \mathcal{R}_p , although such a two-dimensional illustration should be interpreted with caution.

For drug-gene pairs $(d, g) \in \mathcal{R}_p$, we consider the analogy tasks for predicting the target genes g from a drug d . To solve these analogy tasks, we use the relation vector \mathbf{v}_p , which represents the relation between drugs and target genes categorized in the same pathway p . We predict \mathbf{u}_g by adding the relation vector \mathbf{v}_p to \mathbf{u}_d , expecting that

$$\mathbf{u}_d + \mathbf{v}_p \approx \mathbf{u}_g. \quad (13)$$

Equation (13) corresponds to Eq. (4). Therefore, similar to the estimator $\hat{\mathbf{v}}$ in Eq. (7), we define an estimator $\hat{\mathbf{v}}_p$ for the relation vector \mathbf{v}_p as the mean of the vector differences $\mathbf{u}_g - \mathbf{u}_d$ for $(d, g) \in \mathcal{R}_p$:

$$\hat{\mathbf{v}}_p := \mathbb{E}_{\mathcal{R}_p} \{\mathbf{u}_g - \mathbf{u}_d\} = \frac{1}{|\mathcal{R}_p|} \sum_{(d, g) \in \mathcal{R}_p} (\mathbf{u}_g - \mathbf{u}_d), \quad (14)$$

where $\mathbb{E}_{\mathcal{R}_p} \{\cdot\}$ is the sample mean over the set of drug-gene pairs \mathcal{R}_p . For easy comparison with Eq. (5), Eq. (14) is rewritten as the difference of mean vectors:

$$\hat{\mathbf{v}}_p = \mathbb{E}_{\mathcal{R}_p} \{\mathbf{u}_g\} - \mathbb{E}_{\mathcal{R}_p} \{\mathbf{u}_d\}, \quad (15)$$

$$\mathbb{E}_{\mathcal{R}_p} \{\mathbf{u}_g\} = \frac{1}{|\mathcal{R}_p|} \sum_{(d, g) \in \mathcal{R}_p} \mathbf{u}_g, \quad \mathbb{E}_{\mathcal{R}_p} \{\mathbf{u}_d\} = \frac{1}{|\mathcal{R}_p|} \sum_{(d, g) \in \mathcal{R}_p} \mathbf{u}_d. \quad (16)$$

To measure the performance of the estimator $\hat{\mathbf{v}}_p$, we prepare the evaluation of the analogy tasks. Similar to D and G , we define D_p and G_p as the sets of drugs and genes contained in \mathcal{R}_p , respectively. Using the operations of Eq. (10), we define $D_p := \pi_{\mathcal{D}_p}(\mathcal{R}_p) \subset \mathcal{D}_p$ as the set of drugs d such that $(d, g) \in \mathcal{R}_p$ for some genes g , and $G_p := \pi_{\mathcal{G}_p}(\mathcal{R}_p) \subset \mathcal{G}_p$ as the set of genes g such that $(d, g) \in \mathcal{R}_p$ for some drugs d . We also define $[d]_p \subset \mathcal{G}_p$ as the set of genes that have drug-gene relations with a drug $d \in D_p$, and $[g]_p \subset \mathcal{D}_p$ as the set of drugs that have drug-gene relations with a gene $g \in G_p$. Similar to Eq. (11), these sets are formally defined as

$$[d]_p := \{g \mid (d, g) \in \mathcal{R}_p\} \subset \mathcal{G}_p, \quad [g]_p := \{d \mid (d, g) \in \mathcal{R}_p\} \subset \mathcal{D}_p. \quad (17)$$

Given the above, we perform the analogy computation in the following two settings.

Setting P1. For the target genes that have drug-gene relations with a drug d , only genes categorized in the same pathway p as the drug d are considered correct. In other words, for a query drug $d \in D_p$, the set of answer genes is $[d]_p$. The search space is the set of all genes \mathcal{G} , not limited to \mathcal{G}_p , the set of genes categorized in the pathway p . The predicted gene is $\hat{g}_d = \operatorname{argmax}_{g \in \mathcal{G}} \cos(\mathbf{u}_d + \hat{\mathbf{v}}_p, \mathbf{u}_g)$, and if $\hat{g}_d \in [d]_p$, then the prediction is considered correct. We define $\hat{g}_d^{(k)}$ as the k -th ranked $g \in \mathcal{G}$ based on $\cos(\mathbf{u}_d + \hat{\mathbf{v}}_p, \mathbf{u}_g)$. For the top- k accuracy, if $\hat{g}_d^{(k)} \in [d]_p$, then the prediction is considered correct.

Setting P2. The gene predictions \hat{g}_d and $\hat{g}_d^{(k)}$ are defined exactly the same as those in setting P1, but the answer genes are defined the same as in setting G. That is, for the target genes that have drug-gene relations with a drug d , genes are considered correct regardless of whether they are categorized in the same pathway p as the drug d or not. In other words, for a query drug $d \in D$, the set of answer genes is $[d]$, and the prediction is considered correct if $\hat{g}_d \in [d]$. For the top- k accuracy, if $\hat{g}_d^{(k)} \in [d]$, then the prediction is considered correct. Note that the experiment is performed for $d \in \mathcal{D}_p \cap D$ for each p .

Fig. S1 in Supplementary Information 1.1.1 shows the differences between settings P1 and P2 using specific examples. Table S2 in Supplementary Information 1.3 summarizes the queries, answer sets, and search spaces in settings G, P1, and P2.

Analogy tasks for drug-gene pairs by year

In this section, based on analogy tasks for drug-gene pairs, we explain analogy tasks in the setting where datasets are divided by year. In this setting, we can separate the drug-gene relations into *known* or *unknown* relations based on the chronological order they appear within the PubMed abstracts. By training skip-gram embeddings with this dataset, we can test if embeddings of *known* relations have the ability to predict *unknwon* relations. Similar to analogy tasks for drug-gene pairs, we first consider the global setting by year, where all drugs and genes are used in datasets divided by year. Then we consider the pathway-wise setting by year, where drugs and genes are categorized based on pathways in datasets divided by year.

Global setting by year

As a first step, based on analogy tasks for drug-gene pairs, we consider analogy tasks in the global setting, where all drugs and genes are used in datasets divided by year. Specifically, drug-gene relations that appeared up to year y are considered known, while those that appeared after year y are considered unknown. We then train skip-gram embeddings using PubMed abstracts published before the specified year, redefine vectors representing known relations, and use these vectors to predict unknown relations. In preparation, we define y_d as the year when a drug d first appeared in a PubMed abstract, and y_g as the year when a gene g first appeared in a PubMed abstract. In addition, we define $y_{(d,g)}$ as the year when both drug d and gene g first appeared together in a PubMed abstract, and use $y_{(d,g)}$ as a substitute for the year when the relation (d, g) was first identified. By definition, $\max\{y_d, y_g\} \leq y_{(d,g)}$ holds.

Consider a fixed year y . When learning embeddings using PubMed abstracts up to year y as training data, we define $\mathcal{D}^y := \{d \in \mathcal{D} \mid y_d \leq y\}$ and $\mathcal{G}^y := \{g \in \mathcal{G} \mid y_g \leq y\}$ as the sets of drugs and genes that appeared up to year y , respectively. The set of drug-gene pairs that have drug-gene relations and whose drugs and genes appeared up to year y is expressed as

$$\mathcal{R}^y := \{(d, g) \in \mathcal{R} \mid d \in \mathcal{D}^y, g \in \mathcal{G}^y\} \subset \mathcal{D}^y \times \mathcal{G}^y. \quad (18)$$

Since the vocabulary set of the trained embeddings includes both d and g for $(d, g) \in \mathcal{R}^y$, we may discuss this relation (d, g) . The relation (d, g) is interpreted as either known by year y if $y_{(d,g)} \leq y$ or unknown by year y if $y < y_{(d,g)}$.

We divide \mathcal{R}^y into two subsets based on whether $y_{(d,g)} \leq y$ or $y < y_{(d,g)}$. Let us define two intervals, $L_y := (-\infty, y]$ and $U_y := (y, \infty)$. Considering the set for an interval I , consisting of all $(d, g) \in \mathcal{R}^y$ such that $y_{(d,g)} \in I$, i.e.,

$$\mathcal{R}^{y|I} := \{(d, g) \in \mathcal{R}^y \mid y_{(d,g)} \in I\} \subset \mathcal{R}^y, \quad (19)$$

the set of “known” relations is expressed as $\mathcal{R}^{y|L_y}$, and the set of “unknown” relations is expressed as $\mathcal{R}^{y|U_y}$. By definition, $\mathcal{R}^{y|L_y} \cap \mathcal{R}^{y|U_y} = \emptyset$ and $\mathcal{R}^{y|L_y} \cup \mathcal{R}^{y|U_y} = \mathcal{R}^{y|(-\infty, \infty)} = \mathcal{R}^y$.

In analogy tasks, we use ‘‘known’’ $\mathcal{R}^{y|L_y}$ and then predict the target genes g from a drug d for (d, g) in ‘‘unknown’’ $\mathcal{R}^{y|U_y}$. Using the vector \mathbf{v}^y , which represents the drug-gene relations and is derived from $\mathcal{R}^{y|L_y}$, we predict \mathbf{u}_g by adding the relation vector \mathbf{v}^y to \mathbf{u}_d :

$$\mathbf{u}_d + \mathbf{v}^y \approx \mathbf{u}_g. \quad (20)$$

Equation (20) corresponds to Eq. (4). Therefore, similar to the estimator $\hat{\mathbf{v}}$ in Eq. (7), we define an estimator $\hat{\mathbf{v}}^y$ for the relation vector \mathbf{v}^y as the mean of the vector differences $\mathbf{u}_g - \mathbf{u}_d$ for $(d, g) \in \mathcal{R}^{y|L_y}$:

$$\hat{\mathbf{v}}^y := \mathbb{E}_{\mathcal{R}^{y|L_y}} \{ \mathbf{u}_g - \mathbf{u}_d \} = \frac{1}{|\mathcal{R}^{y|L_y}|} \sum_{(d,g) \in \mathcal{R}^{y|L_y}} (\mathbf{u}_g - \mathbf{u}_d), \quad (21)$$

where $\mathbb{E}_{\mathcal{R}^{y|L_y}} \{ \cdot \}$ is the sample mean over the set of drug-gene pairs $\mathcal{R}^{y|L_y}$. For easy comparison with Eq. (5), Eq. (21) is rewritten as the difference of mean vectors:

$$\hat{\mathbf{v}}^y = \mathbb{E}_{\mathcal{R}^{y|L_y}} \{ \mathbf{u}_g \} - \mathbb{E}_{\mathcal{R}^{y|L_y}} \{ \mathbf{u}_d \}, \quad (22)$$

$$\mathbb{E}_{\mathcal{R}^{y|L_y}} \{ \mathbf{u}_g \} = \frac{1}{|\mathcal{R}^{y|L_y}|} \sum_{(d,g) \in \mathcal{R}^{y|L_y}} \mathbf{u}_g, \quad \mathbb{E}_{\mathcal{R}^{y|L_y}} \{ \mathbf{u}_d \} = \frac{1}{|\mathcal{R}^{y|L_y}|} \sum_{(d,g) \in \mathcal{R}^{y|L_y}} \mathbf{u}_d. \quad (23)$$

Given the above, similar to setting G, we perform the analogy tasks in the following two settings.

Setting Y1. For the target genes that have drug-gene relations with a drug d , only genes whose relations appeared after year y are considered correct. In other words, only new discoveries are counted as correct.

Setting Y2. For the target genes that have drug-gene relations with a drug d , these genes are considered correct regardless of whether their relations appeared up to or after year y . In other words, rediscoveries of known relations are also counted as correct.

See Supplementary Information 1.2.1 for more details on these settings. Note that y_d , y_g , and $y_{(d,g)}$ are defined based on the year the drugs, genes, and drug-gene relations appeared in PubMed abstracts. Thus, they do not fully correspond to their actual years of discovery, and we only consider the analogy tasks in these hypothetical settings.

Pathway-wise setting by year

As a next step, based on the analogy tasks in settings P1, P2, Y1, and Y2, we consider more detailed analogy tasks. To do this, we consider the analogy tasks in the pathway-wise setting by year, where drugs and genes are categorized based on pathways in datasets divided by year.

Similar to settings P1, P2, Y1, and Y2, we perform the analogy tasks in the following four settings.

Setting P1Y1. For the target genes that have drug-gene relations with a drug d , only genes categorized in the same pathway p as d , and whose relations appeared after year y , are considered correct.

Setting P1Y2. For the target genes that have drug-gene relations with a drug d , only genes categorized in the same pathway p as the drug d are considered correct, regardless of whether their relations appeared up to or after year y .

Setting P2Y1. For the target genes that have drug-gene relations with a drug d , only genes whose relations appeared after year y are considered correct, regardless of whether they are categorized in the same pathway p as the drug d or not.

Setting P2Y2. For the target genes that have drug-gene relations with a drug d , these genes are considered correct regardless of whether they are categorized in the same pathway or not, and whether their relations appeared up to or after year y .

See Supplementary Information 1.2.2 for details on the analogy tasks and these settings.

Embeddings

BioConceptVec¹³ provides four pretrained 100-dimensional word embeddings: CBOW⁷, skip-gram^{7,8}, GloVe³³, and fastText³⁴. Since CBOW is a simpler model than skip-gram and skip-gram performs better in analogy tasks compared to GloVe⁹, we used BioConceptVec skip-gram embeddings for our experiments. Note that fastText can essentially be considered as a skip-gram using n -grams. To complement the pretrained BioConceptVec embeddings, we further trained 300-dimensional skip-gram embeddings on the publicly available PubMed abstracts. To train our embeddings, we used PubTator¹⁴ to normalize six major biological concepts (genes, mutations, diseases, chemicals, cell lines, and species) in PubMed abstracts, and then tokenized them using NLTK³⁵. Note that since widely used embeddings such as word2vec and GloVe typically have 300 dimensions, we

	BioConceptVec	Ours
$ \mathcal{D} $	117282	28284
$ \mathcal{G} $	144584	51057
$ \mathcal{R} $	6645	5968
$ D $	2262	1980
$ G $	664	634
$E_{d \in D}\{ [d] \}$	2.938	3.014
$E_{g \in G}\{ [g] \}$	10.008	9.413

Table 2. Statistics for setting G.

set the dimensions of our embeddings to 300 instead of the original 100. The hyperparameters used to train our embeddings are shown in Table S4 in Supplementary Information 1.4.

For BioConceptVec and our skip-gram embeddings, Table 2 shows some basic statistics for setting G. Due to the difference in training data size and minimal word occurrence, the sizes of certain sets such as $|\mathcal{D}|$ and $|\mathcal{G}|$ differ significantly between BioConceptVec and our skip-gram embeddings, but the sizes of other sets show somewhat similar trends. Table S1 in Supplementary Information 1.1.1 shows the statistics for settings P1 and P2. The hyperparameters used to train our skip-gram are shown in Table S4 in Supplementary Information 1.4.

Datasets

Corpus Following Chen et al.¹³, we used PubMed (<https://pubmed.ncbi.nlm.nih.gov/>) abstracts to train our skip-gram embeddings. We used about 35 million abstracts up to the year 2023, while they used about 30 million abstracts.

Drug-gene relations For drug-gene relations, we used publicly available data from AsuratDB³⁶, which collects information from various databases including the KEGG¹⁷ database. KEGG (Kyoto Encyclopedia of Genes and Genomes) is a comprehensive database system that integrates a wide range of bioinformatics information such as genomics, chemical reactions, and biological pathways.

Biological Pathways We obtained a list of human pathways from the KEGG API (<https://rest.kegg.jp/list/pathway/hsa>) for use in our experiments. For each pathway, we again used the KEGG API to define sets of drugs and genes. To avoid oversimplification of analogy tasks, we excluded the pathways where only one type of drug or gene had drug-gene relations.

For more details, see Data availability section and Supplementary Information 1.5.

Baseline

To evaluate the performance of predicting target genes by adding the relation vector to a drug embedding, we compare it to a simple baseline method. As a baseline, we randomly select one gene from the search space for each query. We refer to this baseline as the *random baseline*. In the random baseline, we repeated the experiments 10 times and used the average score as the final result.

Evaluation metrics

As evaluation metrics, we use the top- k accuracy explained in each setting, especially the top-1 and top-10 accuracies. We also use Mean Reciprocal Rank (MRR) as another evaluation metric. MRR is a statistical measure to evaluate search performance, expressed as the sum of the reciprocals of the ranks at which the predicted results first appear in the answer set.

When evaluating performance using top-1 accuracy, top-10 accuracy, and MRR, the embeddings of all genes \mathcal{G} (or \mathcal{G}^y in settings by year) are centered using the mean embedding $E_{\mathcal{G}}\{\mathbf{u}_g\}$ in Eq. (6) (or $E_{\mathcal{G}^y}\{\mathbf{u}_g\}$). Since cosine similarity is affected by the origin, centering mitigates this effect. In the case of setting G, for example, we actually calculate the value of $\cos(\mathbf{u}_d + \hat{\mathbf{v}} - E_{\mathcal{G}}\{\mathbf{u}_g\}, \mathbf{u}_g - E_{\mathcal{G}}\{\mathbf{u}_g\})$ instead of $\cos(\mathbf{u}_d + \hat{\mathbf{v}}, \mathbf{u}_g)$.

Results

Gene prediction performance in settings G, P1, and P2. Table 3 shows the results of experiments with BioConceptVec and our skip-gram embeddings in settings G, P1, and P2. In setting G, the prediction by simply adding the global relation vector $\hat{\mathbf{v}}$ resulted in a top-1 accuracy of about 0.3, a top-10 accuracy of over 0.6, and an MRR also over 0.4. These results show that the embeddings have the ability to interpret the drug-gene relations. Similar to the basic analogy task, these relations were

Embeddings	Setting	Method	Metric		
			Top1	Top10	MRR
BioConceptVec	G	Random	0.000	0.000	0.000
		$\hat{\mathbf{v}}$	0.304	0.645	0.419
	P1	Random	0.000	0.000	0.000
		$\hat{\mathbf{v}}_p$	0.499	0.790	0.602
	P2	Random	0.000	0.000	0.000
		$\hat{\mathbf{v}}_p$	0.522	0.807	0.624
Ours	G	Random	0.000	0.000	0.001
		$\hat{\mathbf{v}}$	0.300	0.686	0.426
	P1	Random	0.000	0.001	0.001
		$\hat{\mathbf{v}}_p$	0.589	0.862	0.685
	P2	Random	0.000	0.001	0.001
		$\hat{\mathbf{v}}_p$	0.600	0.880	0.700

Table 3. Gene prediction performance in settings G, P1, and P2.

not explicitly provided during the training of the embeddings. Previous research³⁷ has shown that skip-gram achieves a top-1 accuracy of 0.56 on the Microsoft Research Syntactic Analogies Dataset³⁸. Given this, BioConceptVec and our skip-gram embeddings in the analogy tasks for drug-gene pairs show comparable performance to skip-gram in the basic analogy tasks.

In settings P1 and P2, prediction by adding the pathway-wise relation vector $\hat{\mathbf{v}}_p$ showed better performance than in setting G. For example, our skip-gram embeddings achieved a top-1 accuracy of over 0.5 in both settings P1 and P2. This is probably because the queries are specific drugs categorized in some pathways, and we use the pathway information to calculate the relation vectors. Since the analogy tasks are considered for each pathway, these settings are also likely to make the tasks easier than those in setting G.

In contrast, the random baseline in settings G, P1, and P2 showed nearly zero scores for all evaluation metrics, suggesting that random prediction is nearly impossible in these analogy tasks. This also confirms the superior performance of prediction by adding relation vectors.

In addition, our skip-gram outperformed BioConceptVec except for the top-1 accuracy in setting G. This is probably because BioConceptVec has a dimensionality of 100, while our skip-gram has a dimensionality of 300. Note that, as shown in Table 2, the settings of the analogy tasks are not identical for these two embeddings.

For the results in Table 3, we used the better estimators in equations (7) and (14), not the naive estimators in equations (5) and (S1), and calculated the cosine similarities after centering the embeddings of all genes \mathcal{G} (or \mathcal{G}'). The results of the naive estimators and the centering ablation study are shown in Table S5 in Supplementary Information 2.1.1. The results of the analogy tasks for predicting drugs from a query gene are shown in Table S6 in Supplementary Information 2.1.2.

Gene prediction performance in settings Y1 and Y2 Figures 3a and 3b show the results of experiments with our skip-gram embeddings in settings Y1 and Y2. BioConceptVec embeddings are not appropriate for the settings by year, since they are pretrained on the entire dataset without year-specific divisions.

In setting Y1, since only genes whose relations appeared after year y are included in the answer set, the tasks are more challenging. Therefore, the evaluation metric scores are lower compared to those in setting Y2, where genes whose relations appeared up to year y are also included in the answer set. Yet, in setting Y1, the top-1 accuracy from $y = 1985$ to $y = 2015$ is about 0.1, the top-10 accuracy is over 0.3, and the MRR is about 0.2. Although in setting Y1 the relations to be predicted appeared after year y and are not used to calculate $\hat{\mathbf{v}}^y$, these results show that adding $\hat{\mathbf{v}}^y$ to \mathbf{u}_d can predict these relations. Setting Y2 is easier than setting Y1, and using the relation vectors results in high evaluation metric scores. For example, from $y = 1985$ to $y = 2015$, the top-1 accuracy reaches about 0.3, and the top-10 accuracy is about 0.7.

In setting Y1, the number of queries increases initially and then decreases over time, while in setting Y2, the number of queries increases steadily from older to more recent years. In addition, the size of the search space is small for older years (e.g., $|\mathcal{G}^{1970}| = 353$) and increases for later years (e.g., $|\mathcal{G}^{2020}| = 47509$). As a result, in both settings Y1 and Y2, the datasets for older years such as $y = 1970, 1975$, and 1980 have fewer queries and smaller search spaces, resulting in unusually high evaluation metric scores. In setting Y1, the datasets for later years have fewer queries and larger search spaces, which tends to produce lower evaluation metric scores. In both settings, the evaluation metric scores for the random baseline are close to zero. For more detailed results for settings Y1 and Y2, see Table S8 in Supplementary Information 2.2.1.

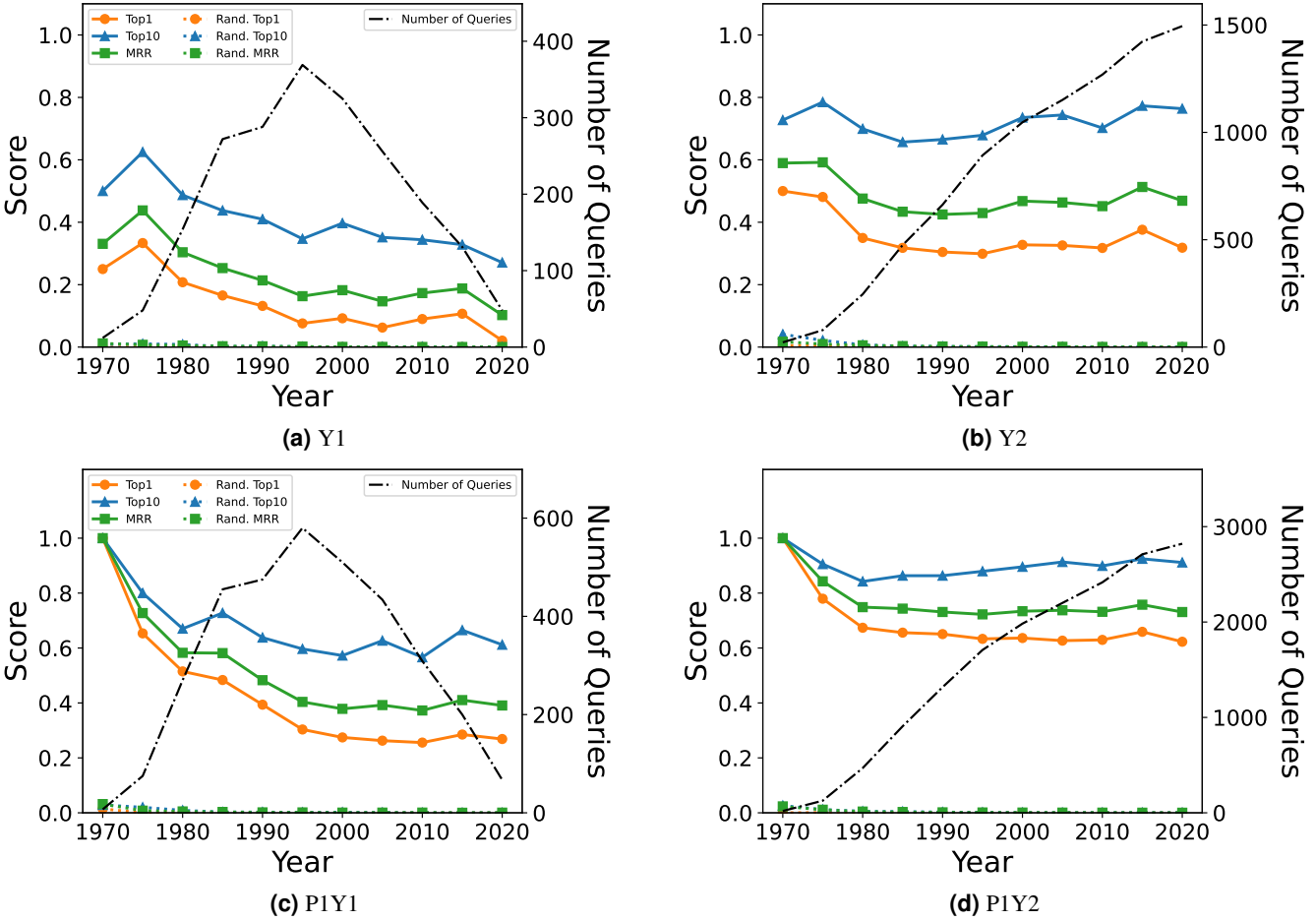


Figure 3. Gene prediction performance and the number of queries for each year in settings Y1, Y2, P1Y1, and P1Y2.

Gene prediction performance in settings P1Y1, P1Y2, P2Y1 and P2Y2. Figures 3c and 3d show the results of experiments with our skip-gram embeddings in settings P1Y1 and P1Y2. The results in settings P1Y1 and P1Y2 not only follow similar trends to those in settings Y1 and Y2 but also consistently show higher evaluation metric scores. The analogy tasks in settings P1Y1 and P1Y2 use detailed pathway information. Therefore, predicting the relations that appeared after year y is easier in settings P1Y1 and P1Y2 than in settings Y1 and Y2. In addition, the results for the older years show extremely high evaluation metric scores in settings P1Y1 and P1Y2, similar to those in settings Y1 and Y2. The evaluation metric scores of the random baseline are close to zero.

For the results in settings P2Y1 and P2Y2, see Fig. S2 in Supplementary Information 2.2.2. They are very similar to those in settings P1Y1 and P1Y2. For detailed results for settings P1Y1, P1Y2, P2Y1, and P2Y2, see Table S10 in Supplementary Information 2.2.2.

Discussion

In this section, we investigate the predictions made by adding the relation vector in settings G, P1, and P2. For this purpose, we focus on the results using genes and drugs categorized in the *ErbB signaling pathway* as shown in Table 1 and Fig. 2b. Furthermore, since our skip-gram embeddings showed better performance compared to the BioConceptVec skip-gram embeddings (Table 3), we adopted our embeddings for this analysis. \mathcal{D}_p , \mathcal{G}_p , and \mathcal{R}_p of our embeddings are identical to those of the BioConceptVec embeddings in Table 1.

In Table 4, we list the predicted target genes for drugs that are categorized in the *ErbB signaling pathway* and whose answer set size in setting G is two or more. For all drugs meeting these criteria, at least one answer gene was included in the top 10 predicted target genes for either of the settings. In the following, we show that genes that were ranked high in the predictions, even though they were not in the answer set, can be interpreted biologically.

First, the target genes of Bosutinib are ABL1 and SRC, which are both known to be non-receptor tyrosine kinases (non-

Drug	Setting	Gene Prediction										Answer Set
		Top1	Top2	Top3	Top4	Top5	Top6	Top7	Top8	Top9	Top10	
Bosutinib	G	<u>ABL1</u>	TXK	BCR	BTK	PDGFRB	FYN	FLT3	HCK	KIT	CSK	{ABL1, SRC}
	P1	<u>ABL1</u>	TXK	EGFR	BCR	ALK	RUNX1	FLT3	KIT	JAK2	ERBB2	{ABL1, SRC}
	P2	<u>ABL1</u>	TXK	EGFR	BCR	ALK	RUNX1	FLT3	KIT	JAK2	ERBB2	{ABL1, SRC}
Canertinib dihydrochloride	G	TTK	CHRM5	CEP72	TOP2A	AURKB	PTTG1	—	AKAP6	CENPE	FPGS	{EGFR, ERBB2, ERBB3, ERBB4}
	P1	<u>ERBB2</u>	EGFR	BRAF	ALK	MET	CTLA4	AR	MDM2	TOP2A	PGR	{EGFR, ERBB2, ERBB3, ERBB4}
	P2	<u>ERBB2</u>	EGFR	BRAF	ALK	MET	CTLA4	AR	MDM2	TOP2A	PGR	{EGFR, ERBB2, ERBB3, ERBB4}
Dacomitinib	G	ERBB3	ROS1	EGFR	FGFR2	ALK	EML4	MET	BTK	TXK	<u>ERBB4</u>	{EGFR, ERBB2, ERBB4}
	P1	EGFR	ALK	ROS1	<u>ERBB2</u>	ERBB3	KRAS	MET	BRAF	PIK3CA	TXK	{EGFR, ERBB2, ERBB4}
	P2	EGFR	ALK	ROS1	<u>ERBB2</u>	ERBB3	KRAS	MET	BRAF	PIK3CA	TXK	{EGFR, ERBB2, ERBB4}
Masoprolol	G	ALOX5	ALOX12	PTGS2	—	PTGS1	ALOX15B	—	PTGES	COMT	HDAC6	{EGFR, IGF1}
	P1	ALOX5	ERBB2	TP53	PTGS2	EGFR	HSP90AA1	TERT	COX2	EREG	GSK3A	{EGFR}
	P2	ALOX5	ERBB2	TP53	PTGS2	EGFR	HSP90AA1	TERT	COX2	EREG	GSK3A	{EGFR, IGF1}
Neratinib	G	ERBB3	CDK6	ESR1	PDGFR	ROS1	CDK4	EREG	ERBB2	PIK3CA	<u>ERBB4</u>	{EGFR, ERBB2, ERBB4}
	P1	<u>ERBB2</u>	EGFR	ESR1	EREG	ERBB3	NR4A1	PGK	ROS1	PIK3CA	ERBB4	{EGFR, ERBB2, ERBB4}
	P2	<u>ERBB2</u>	EGFR	ESR1	EREG	ERBB3	NR4A1	PGK	ROS1	PIK3CA	ERBB4	{EGFR, ERBB2, ERBB4}
Nilotinib	G	<u>ABL1</u>	BCR	FYN	KIT	PDGFR	FLT3	TXK	BTK	PDE10A	RUNX1	{ABL1, PDGFR, PDGFRB, KIT}
	P1	<u>ABL1</u>	EGFR	ERBB2	BRAF	ALK	RUNX1	KIT	KRAS	JAK2	BCR	{ABL1, PDGFR, PDGFRB, KIT}
	P2	<u>ABL1</u>	EGFR	ERBB2	BRAF	ALK	RUNX1	KIT	KRAS	JAK2	BCR	{ABL1, PDGFR, PDGFRB, KIT}
Pimasertib	G	<u>MAP2K2</u>	PIK3CB	CDK4	PIK3R1	—	CDK6	PIK3CD	<u>MAP2K1</u>	GRM3	MAP2K7	{MAP2K1, MAP2K2}
	P1	EGFR	BRAF	<u>MAP2K2</u>	MAP2K7	MAP2K1	CDK4	MET	ERBB2	NRAS	KRAS	{MAP2K1, MAP2K2}
	P2	EGFR	BRAF	<u>MAP2K2</u>	MAP2K7	MAP2K1	CDK4	MET	ERBB2	NRAS	KRAS	{MAP2K1, MAP2K2}
Pozotinib	G	ERBB3	EML4	FGFR2	ROS1	PIK3CA	ALK	MET	ERBB4	FGR4	NRAS	{EGFR, ERBB2}
	P1	EGFR	ERBB2	ERBB3	ROS1	ALK	PIK3CA	MET	NRAS	FGR2	MAP2K7	{EGFR, ERBB2}
	P2	EGFR	ERBB2	ERBB3	ROS1	ALK	PIK3CA	MET	NRAS	FGR2	MAP2K7	{EGFR, ERBB2}
Saracatinib	G	FYN	DDR1	ERBB4	DRD4	GRM3	GRIN2B	CHRNN7	GRIN2A	EPAH3	SLC6A9	{ABL1, SRC}
	P1	EGFR	ERBB4	ERBB2	SRC	ESR1	MAPK1	STAT3	MET	KDR	PTK2	{ABL1, SRC}
	P2	EGFR	ERBB4	ERBB2	SRC	ESR1	MAPK1	STAT3	MET	KDR	PTK2	{ABL1, SRC}
Selumetinib	G	MAP2K7	<u>MAP2K2</u>	CDK4	RAF1	PIK3CA	PIK3R1	<u>MAP2K1</u>	CDK6	NRAS	BRAF	{MAP2K1, MAP2K2}
	P1	MAP2K7	BRAF	PIK3CA	KRAS	MAP2K1	EGFR	NRAS	CDK4	MAPK1	PTEN	{MAP2K1, MAP2K2}
	P2	MAP2K7	BRAF	PIK3CA	KRAS	MAP2K1	EGFR	NRAS	CDK4	MAPK1	PTEN	{MAP2K1, MAP2K2}
Tozasertib	G	SCN9A	INCENP	CDC25C	AURKC	AURKB	PLXNA1	NEK6	KDM5A	KIF20A	MYT1	{AURKA, AURKB, AURKC, ABL1, FLT3}
	P1	AURKA	SRC	CHEK1	<u>ABL1</u>	PLK1	WEE1	CDK2	CASP3	BRD4	MAP2K1	{ABL1}
	P2	AURKA	SRC	CHEK1	<u>ABL1</u>	PLK1	WEE1	CDK2	CASP3	BRD4	MAP2K1	{AURKA, AURKB, AURKC, ABL1, FLT3}
Trametinib	G	MAP2K7	<u>MAP2K2</u>	CDK6	CDK4	<u>MAP2K1</u>	RAF1	MAPK1	BRAF	MAPK3	PIK3CA	{MAP2K1, MAP2K2}
	P1	MAP2K7	EGFR	BRAF	MAPK1	KRAS	MAP2K1	MAPK3	CDK4	CD274	CDK6	{MAP2K1, MAP2K2}
	P2	MAP2K7	EGFR	BRAF	MAPK1	KRAS	MAP2K1	MAPK3	CDK4	CD274	CDK6	{MAP2K1, MAP2K2}
Vandetanib	G	KDR	TSHR	RET	FLT4	TXK	VEGFA	IGF1R	FLT1	AXL	PIK3CA	{EGFR, KDR, RET}
	P1	EGFR	KDR	BRAF	RET	VEGFA	IGF1R	MAPK3	ERBB2	MET	MAPK1	{EGFR}
	P2	EGFR	KDR	BRAF	RET	VEGFA	IGF1R	MAPK3	ERBB2	MET	MAPK1	{EGFR, KDR, RET}
Varlitinib	G	ERBB3	—	PPFIBP2	MIR4656	MIR4323	MIR1181	EFNA4	LY6G6D	CDH10	SLC39A11	{EGFR, ERBB2, ERBB4}
	P1	ERBB3	EGFR	<u>ERBB2</u>	ERBB4	ESR1	KRAS	CD274	MET	EREG	ROS1	{EGFR, ERBB2, ERBB4}
	P2	ERBB3	EGFR	<u>ERBB2</u>	ERBB4	ESR1	KRAS	CD274	MET	EREG	ROS1	{EGFR, ERBB2, ERBB4}

Table 4. Gene prediction results for the drugs categorized in the *ErbB signaling pathway*. Shown only for drugs where the size of $[d]$ is two or more. For each drug, the top ten predicted genes and their answer sets are shown in settings G, P1, and P2. Predicted genes included in the answer sets are underlined. Genes whose IDs could not be converted to gene names are indicated by “—”.

RTKs³⁹. Within the top 10 predicted target genes, TXK⁴⁰ and JAK2⁴¹ can also be categorized as non-RTKs, sharing some properties with ABL1 and SRC. This implies that the structural and biochemical similarities of these genes may have been reflected in their high-dimensional representations.

For Masoprolol, we were able to predict the correct target gene EGFR as the fifth prediction in settings P1 and P2. However, although EGFR is the sole target gene of Masoprolol according to the information deposited in KEGG, it is also reported to have inhibitory effects towards lipoxygenase activity⁴². Since ALOX5 is a gene that codes a lipoxygenase, treating this prediction as inaccurate should be considered incorrect. The diseases in which Masoprolol is used for its treatment include actinic keratosis⁴³, and it has been previously known that the mutation of TP53 is involved in the onset of this disease^{44,45}. Also, the gene that was ranked the highest in this setting, ALOX5, is reported to be one of the transcription targets of TP53⁴⁶. Taken together, this information suggests that TP53 is deeply related to the target gene and symptoms of Masoprolol, and therefore, although it may not be a direct target, it was highly ranked in the prediction.

When we set Pozotinib as the query, EGFR and ERBB2 were correctly ranked the highest in settings P1 and P2. However, in setting G, ROS1, EML4, and ALK were also found among the highly ranked targets. Since Pozotinib was initially developed as an effective drug to treat lung cancer with HER2 mutation⁴⁷, it can be interpreted that such context was reflected in the embeddings, as ROS1 and EML4-ALK fusion genes are also characteristic mutations and therapeutic targets in lung cancer^{48,49}.

Selumetinib and Trametinib both target MAP2K1 and MAP2K2, and in both cases these genes were found within the top 10 predictions. Aside from these target genes, we observed BRAF and PI3KCA placed in higher rank among the predicted genes. Considering the history that these drugs were both developed for treating cancers with BRAF V600 mutation and that combination treatment with inhibition of the PI3K-AKT pathway have been explored⁵⁰⁻⁵², we assumed that such background was reflected in these results.

As we explored in this section, it was suggested that the high-dimensional representations of genes and drugs calculated from biomedical texts not only capture the simple drug-gene relations we sought to predict in this study, but also integrate broader higher-order information. In this specific analysis, predicted genes are closely related to the genes or symptoms that have direct molecular interactions with the target genes, or those that are alternative therapeutic targets for the target disease.

Conclusions

In this study, we used the embeddings learned from biological texts and performed analogy tasks for predicting drug-gene relations. We defined vectors representing these relations and showed that these vectors can accurately predict the target genes for given drugs. Furthermore, we categorized drugs and genes based on biological pathways and then defined vectors representing drug-gene relations for each pathway. Analogy computation using these vectors showed more performance improvement. In addition, we divided datasets by year and redefined the vectors representing known relations to predict unknown relations. The experimental results show that our approach can predict unknown relations to some extent.

Data availability

Corpus

PubMed abstracts is available at <https://ftp.ncbi.nlm.nih.gov/pubmed/>.

Embeddings

word2vec is available at <https://code.google.com/archive/p/word2vec/>. BioConceptVec¹³ is available at <https://github.com/ncbi/BioConceptVec>.

Drug-gene relations

The published data from AsuratDB³⁶, which is based on the KEGG database⁵³, is available at https://github.com/keita-iida/ASURATDB/blob/main/genes2bioterm/20221102_human_KEGG_drug.rda. The drug-gene relations used in this study are published with our code.

Pathways

A list of pathways is available at <https://rest.kegg.jp/list/pathway/hsa>. For each pathway, drug and gene sets are available. For example, the sets of drugs and genes categorized in the *ErbB signaling pathway*, whose pathway ID is hsa04012, are available at <https://rest.kegg.jp/get/hsa04012>.

Code availability

Our code is available at <https://github.com/shimo-lab/Drug-Gene-Analogy>.

References

1. Vaswani, A. *et al.* Attention is all you need. In Guyon, I. *et al.* (eds.) *Advances in Neural Information Processing Systems*, vol. 30 (Curran Associates, Inc., 2017).
2. Raffel, C. *et al.* Exploring the limits of transfer learning with a unified text-to-text transformer. *J. Mach. Learn. Res.* **21**, 140:1–140:67 (2020).
3. Socher, R. *et al.* Recursive deep models for semantic compositionality over a sentiment treebank. In *Proceedings of the 2013 Conference on Empirical Methods in Natural Language Processing, EMNLP 2013, 18-21 October 2013, Grand Hyatt Seattle, Seattle, Washington, USA, A meeting of SIGDAT, a Special Interest Group of the ACL*, 1631–1642 (ACL, 2013).
4. Devlin, J., Chang, M.-W., Lee, K. & Toutanova, K. BERT: Pre-training of deep bidirectional transformers for language understanding. In *Proceedings of the 2019 Conference of the North American Chapter of the Association for Computational Linguistics: Human Language Technologies, Volume 1 (Long and Short Papers)*, 4171–4186, DOI: [10.18653/v1/N19-1423](https://doi.org/10.18653/v1/N19-1423) (Association for Computational Linguistics, Minneapolis, Minnesota, 2019).
5. Cer, D., Diab, M., Agirre, E., Lopez-Gazpio, I. & Specia, L. SemEval-2017 task 1: Semantic textual similarity multilingual and crosslingual focused evaluation. In *Proceedings of the 11th International Workshop on Semantic Evaluation (SemEval-2017)*, 1–14, DOI: [10.18653/v1/S17-2001](https://doi.org/10.18653/v1/S17-2001) (Association for Computational Linguistics, Vancouver, Canada, 2017).
6. Mu, J. & Viswanath, P. All-but-the-top: Simple and effective postprocessing for word representations. In *6th International Conference on Learning Representations, ICLR 2018, Vancouver, BC, Canada, April 30 - May 3, 2018, Conference Track Proceedings* (OpenReview.net, 2018).

7. Mikolov, T., Chen, K., Corrado, G. & Dean, J. Efficient estimation of word representations in vector space. In Bengio, Y. & LeCun, Y. (eds.) *1st International Conference on Learning Representations, ICLR 2013, Scottsdale, Arizona, USA, May 2-4, 2013, Workshop Track Proceedings* (2013).
8. Mikolov, T., Sutskever, I., Chen, K., Corrado, G. S. & Dean, J. Distributed representations of words and phrases and their compositionality. In Burges, C. J. C., Bottou, L., Ghahramani, Z. & Weinberger, K. Q. (eds.) *Advances in Neural Information Processing Systems 26: 27th Annual Conference on Neural Information Processing Systems 2013. Proceedings of a meeting held December 5-8, 2013, Lake Tahoe, Nevada, United States*, 3111–3119 (2013).
9. Allen, C. & Hospedales, T. Analogies explained: Towards understanding word embeddings. In Chaudhuri, K. & Salakhutdinov, R. (eds.) *Proceedings of the 36th International Conference on Machine Learning*, vol. 97 of *Proceedings of Machine Learning Research*, 223–231 (PMLR, 2019).
10. Lee, J. *et al.* Biobert: a pre-trained biomedical language representation model for biomedical text mining. *Bioinform.* **36**, 1234–1240, DOI: [10.1093/bioinformatics/btz682](https://doi.org/10.1093/bioinformatics/btz682) (2020).
11. Giorgi, J., Bader, G. & Wang, B. A sequence-to-sequence approach for document-level relation extraction. In *Proceedings of the 21st Workshop on Biomedical Language Processing*, 10–25, DOI: [10.18653/v1/2022.bionlp-1.2](https://doi.org/10.18653/v1/2022.bionlp-1.2) (Association for Computational Linguistics, Dublin, Ireland, 2022).
12. Luo, R. *et al.* Biogpt: generative pre-trained transformer for biomedical text generation and mining. *Briefings Bioinform.* **23**, DOI: [10.1093/bib/bbac409](https://doi.org/10.1093/bib/bbac409) (2022).
13. Chen, Q. *et al.* Bioconceptvec: Creating and evaluating literature-based biomedical concept embeddings on a large scale. *PLoS Comput. Biol.* **16**, DOI: [10.1371/journal.pcbi.1007617](https://doi.org/10.1371/journal.pcbi.1007617) (2020).
14. Wei, C., Kao, H. & Lu, Z. Pubtator: a web-based text mining tool for assisting biocuration. *Nucleic Acids Res.* **41**, 518–522, DOI: [10.1093/nar/gkt441](https://doi.org/10.1093/nar/gkt441) (2013).
15. Sachdev, K. & Gupta, M. K. A comprehensive review of feature based methods for drug target interaction prediction. *J. biomedical informatics* **93**, 103159 (2019).
16. Djeddi, W. E., Hermi, K., Ben Yahia, S. & Diallo, G. Advancing drug–target interaction prediction: a comprehensive graph-based approach integrating knowledge graph embedding and protbert pretraining. *BMC bioinformatics* **24**, 488 (2023).
17. Ogata, H. *et al.* Kegg: Kyoto encyclopedia of genes and genomes. *Nucleic Acids Res* **27**, 29–34, DOI: [10.1093/nar/27.1.29](https://doi.org/10.1093/nar/27.1.29) (1999).
18. Tshitoyan, V. *et al.* Unsupervised word embeddings capture latent knowledge from materials science literature. *Nat.* **571**, 95–98, DOI: [10.1038/s41586-019-1335-8](https://doi.org/10.1038/s41586-019-1335-8) (2019).
19. Shtar, G., Greenstein-Messica, A., Mazuz, E., Rokach, L. & Shapira, B. Predicting drug characteristics using biomedical text embedding. *BMC Bioinforma.* **23**, 526, DOI: [10.1186/s12859-022-05083-1](https://doi.org/10.1186/s12859-022-05083-1) (2022).
20. Alachram, H., Chereda, H., Beißbarth, T., Wingender, E. & Stegmaier, P. Text mining-based word representations for biomedical data analysis and protein–protein interaction networks in machine learning tasks. *PLOS ONE* **16**, 1–20, DOI: [10.1371/journal.pone.0258623](https://doi.org/10.1371/journal.pone.0258623) (2021).
21. Liu, S., Tang, B., Chen, Q. & Wang, X. Drug-drug interaction extraction via convolutional neural networks. *Comput. Math. Methods Medicine* **2016**, 6918381, DOI: [10.1155/2016/6918381](https://doi.org/10.1155/2016/6918381) (2016).
22. Sahu, S. K. & Anand, A. Drug-drug interaction extraction from biomedical texts using long short-term memory network. *J Biomed Inf.* **86**, 15–24 (2018).
23. Jiang, Z., Li, L. & Huang, D. A general protein-protein interaction extraction architecture based on word representation and feature selection. *Int. J. Data Min. Bioinforma.* **14**, 276–291, DOI: [10.1504/IJDMB.2016.074878](https://doi.org/10.1504/IJDMB.2016.074878) (2016). <https://www.inderscienceonline.com/doi/pdf/10.1504/IJDMB.2016.074878>.
24. Quan, C., Luo, Z. & Wang, S. A hybrid deep learning model for protein–protein interactions extraction from biomedical literature. *Appl. Sci.* **10**, DOI: [10.3390/app10082690](https://doi.org/10.3390/app10082690) (2020).
25. Zhang, Y. *et al.* A hybrid model based on neural networks for biomedical relation extraction. *J. Biomed. Informatics* **81**, 83–92, DOI: <https://doi.org/10.1016/j.jbi.2018.03.011> (2018).
26. Müller, H.-M., Kenny, E. E. & Sternberg, P. W. Textpresso: An ontology-based information retrieval and extraction system for biological literature. *PLOS Biol.* **2**, null, DOI: [10.1371/journal.pbio.0020309](https://doi.org/10.1371/journal.pbio.0020309) (2004).

27. Friedman, C., Kra, P., Yu, H., Krauthammer, M. & Rzhetsky, A. GENIES: a natural-language processing system for the extraction of molecular pathways from journal articles. *Bioinformatics* **17 Suppl 1**, S74–82 (2001).
28. Yeganova, L. *et al.* Better synonyms for enriching biomedical search. *J. Am. Med. Informatics Assoc.* **27**, 1894–1902, DOI: [10.1093/jamia/ocaa151](https://doi.org/10.1093/jamia/ocaa151) (2020). <https://academic.oup.com/jamia/article-pdf/27/12/1894/34838591/ocaa151.pdf>.
29. Du, J. *et al.* Gene2vec: distributed representation of genes based on co-expression. *BMC Genomics* **20**, 82, DOI: [10.1186/s12864-018-5370-x](https://doi.org/10.1186/s12864-018-5370-x) (2019).
30. Peng, Y., Yan, S. & Lu, Z. Transfer learning in biomedical natural language processing: An evaluation of BERT and ELMo on ten benchmarking datasets. In *Proceedings of the 18th BioNLP Workshop and Shared Task*, 58–65, DOI: [10.18653/v1/W19-5006](https://doi.org/10.18653/v1/W19-5006) (Association for Computational Linguistics, Florence, Italy, 2019).
31. Fang, L., Chen, Q., Wei, C.-H., Lu, Z. & Wang, K. Bioformer: an efficient transformer language model for biomedical text mining (2023). [2302.01588](https://doi.org/10.48550/2302.01588).
32. Kutuzov, A., Velldal, E. & Øvreliid, L. One-to-X analogical reasoning on word embeddings: a case for diachronic armed conflict prediction from news texts. In Tahmasebi, N., Borin, L., Jatowt, A. & Xu, Y. (eds.) *Proceedings of the 1st International Workshop on Computational Approaches to Historical Language Change*, 196–201, DOI: [10.18653/v1/W19-4724](https://doi.org/10.18653/v1/W19-4724) (Association for Computational Linguistics, Florence, Italy, 2019).
33. Pennington, J., Socher, R. & Manning, C. D. Glove: Global vectors for word representation. In Moschitti, A., Pang, B. & Daelemans, W. (eds.) *Proceedings of the 2014 Conference on Empirical Methods in Natural Language Processing, EMNLP 2014, October 25-29, 2014, Doha, Qatar, A meeting of SIGDAT, a Special Interest Group of the ACL*, 1532–1543, DOI: [10.3115/v1/d14-1162](https://doi.org/10.3115/v1/d14-1162) (ACL, 2014).
34. Bojanowski, P., Grave, E., Joulin, A. & Mikolov, T. Enriching word vectors with subword information. *Trans. Assoc. Comput. Linguist.* **5**, 135–146, DOI: [10.1162/tacl_a_00051](https://doi.org/10.1162/tacl_a_00051) (2017).
35. Bird, S. & Loper, E. NLTK: The natural language toolkit. In *Proceedings of the ACL Interactive Poster and Demonstration Sessions*, 214–217 (Association for Computational Linguistics, Barcelona, Spain, 2004).
36. Iida, K., Kondo, J., Wibisana, J. N., Inoue, M. & Okada, M. ASURAT: functional annotation-driven unsupervised clustering of single-cell transcriptomes. *Bioinformatics* **38**, 4330–4336, DOI: [10.1093/bioinformatics/btac541](https://doi.org/10.1093/bioinformatics/btac541) (2022). <https://academic.oup.com/bioinformatics/article-pdf/38/18/4330/45878308/btac541.pdf>.
37. Mikolov, T., Chen, K., Corrado, G. & Dean, J. Efficient estimation of word representations in vector space. In Bengio, Y. & LeCun, Y. (eds.) *1st International Conference on Learning Representations, ICLR 2013, Scottsdale, Arizona, USA, May 2-4, 2013, Workshop Track Proceedings* (2013).
38. Mikolov, T., Yih, W. & Zweig, G. Linguistic regularities in continuous space word representations. In Vanderwende, L., III, H. D. & Kirchhoff, K. (eds.) *Human Language Technologies: Conference of the North American Chapter of the Association of Computational Linguistics, Proceedings, June 9-14, 2013, Westin Peachtree Plaza Hotel, Atlanta, Georgia, USA*, 746–751 (The Association for Computational Linguistics, 2013).
39. Siveen, K. S. *et al.* Role of Non Receptor Tyrosine Kinases in Hematological Malignancies and its Targeting by Natural Products. *Mol. Cancer* **17**, 31, DOI: [10.1186/s12943-018-0788-y](https://doi.org/10.1186/s12943-018-0788-y) (2018).
40. Maruyama, T., Nara, K., Yoshikawa, H. & Suzuki, N. Tlxk, a member of the non-receptor tyrosine kinase of the Tec family, forms a complex with poly(ADP-ribose) polymerase 1 and elongation factor 1 α and regulates interferon- γ gene transcription in Th1 cells. *Clin. Exp. Immunol.* **147**, 164–175, DOI: [10.1111/j.1365-2249.2006.03249.x](https://doi.org/10.1111/j.1365-2249.2006.03249.x) (2007).
41. Hu, X., Li, J., Fu, M., Zhao, X. & Wang, W. The JAK/STAT signaling pathway: From bench to clinic. *Signal Transduct. Target. Ther.* **6**, 1–33, DOI: [10.1038/s41392-021-00791-1](https://doi.org/10.1038/s41392-021-00791-1) (2021).
42. Tappel, A. L., Lundberg, W. O. & Boyer, P. D. Effect of temperature and antioxidants upon the lipoxidase-catalyzed oxidation of sodium linoleate. *Arch. Biochem. Biophys.* **42**, 293–304, DOI: [10.1016/0003-9861\(53\)90359-2](https://doi.org/10.1016/0003-9861(53)90359-2) (1953).
43. Callen, J. P., Bickers, D. R. & Moy, R. L. Actinic keratoses. *J. Am. Acad. Dermatol.* **36**, 650–653, DOI: [10.1016/S0190-9622\(97\)70265-2](https://doi.org/10.1016/S0190-9622(97)70265-2) (1997).
44. Park, W.-s. *et al.* P53 mutations in solar keratoses. *Hum. Pathol.* **27**, 1180–1184, DOI: [10.1016/S0046-8177\(96\)90312-3](https://doi.org/10.1016/S0046-8177(96)90312-3) (1996).
45. Brash, D. E. Roles of the transcription factor p53 in keratinocyte carcinomas. *Br. J. Dermatol.* **154**, 8–10, DOI: [10.1111/j.1365-2133.2006.07230.x](https://doi.org/10.1111/j.1365-2133.2006.07230.x) (2006).
46. Gilbert, B. *et al.* 5-Lipoxygenase is a direct p53 target gene in humans. *Biochimica et Biophys. Acta (BBA) - Gene Regul. Mech.* **1849**, 1003–1016, DOI: [10.1016/j.bbagen.2015.06.004](https://doi.org/10.1016/j.bbagen.2015.06.004) (2015).

47. Elamin, Y. Y. *et al.* Pozotinib for *EGFR* exon 20-mutant NSCLC: Clinical efficacy, resistance mechanisms, and impact of insertion location on drug sensitivity. *Cancer Cell* **40**, 754–767.e6, DOI: [10.1016/j.ccr.2022.06.006](https://doi.org/10.1016/j.ccr.2022.06.006) (2022).
48. Davies, K. D. *et al.* Identifying and Targeting *ROS1* Gene Fusions in Non-Small Cell Lung Cancer. *Clin. Cancer Res.* **18**, 4570–4579, DOI: [10.1158/1078-0432.CCR-12-0550](https://doi.org/10.1158/1078-0432.CCR-12-0550) (2012).
49. Sasaki, T., Rodig, S. J., Chirieac, L. R. & Jänne, P. A. The biology and treatment of *EML4-ALK* non-small cell lung cancer. *Eur. J. Cancer* **46**, 1773–1780, DOI: [10.1016/j.ejca.2010.04.002](https://doi.org/10.1016/j.ejca.2010.04.002) (2010).
50. US Food and Drug Administration. Fda approves dabrafenib plus trametinib for adjuvant treatment of melanoma with braf v600e or v600k mutations (2018).
51. Patel, S. P. & Kim, K. B. Selumetinib (AZD6244; ARRY-142886) in the treatment of metastatic melanoma. *Expert. Opin. on Investig. Drugs* **21**, 531–539, DOI: [10.1517/13543784.2012.665871](https://doi.org/10.1517/13543784.2012.665871) (2012).
52. Tolcher, A. W. *et al.* A phase I dose-escalation study of oral MK-2206 (allosteric AKT inhibitor) with oral selumetinib (AZD6244; MEK inhibitor) in patients with advanced or metastatic solid tumors. *J. Clin. Oncol.* **29**, 3004–3004, DOI: [10.1200/jco.2011.29.15_suppl.3004](https://doi.org/10.1200/jco.2011.29.15_suppl.3004) (2011).
53. Kanehisa, M., Goto, S., Furumichi, M., Tanabe, M. & Hirakawa, M. KEGG for representation and analysis of molecular networks involving diseases and drugs. *Nucleic Acids Res.* **38**, 355–360, DOI: [10.1093/nar/gkp896](https://doi.org/10.1093/nar/gkp896) (2010).
54. Maglott, D., Ostell, J., Pruitt, K. D. & Tatusova, T. Entrez gene: gene-centered information at ncbi. *Nucleic acids research* **33**, D54–D58 (2005).

Acknowledgements

This study was partially supported by JSPS KAKENHI 22H05106, 23H03355, JST CREST JPMJCR21N3, JST SPRING JPMJSP2110.

Author contributions statement

H.Y., R.H., K.A., Ma.O. and H.S. conceived the experiments, H.Y., R.H., K.A., and K.M. conducted the experiments, H.Y., R.H., K.A., K.M., S.S., Ma.O., and H.S. analysed the results, R.H. and Mo.O. surveyed existing research. All authors reviewed the manuscript.

Supplementary Information

1 Details of analogy tasks

1.1 Analogy tasks for drug-gene pairs.

1.1.1 Pathway-wise setting

In Eq. (14), the estimator $\hat{\mathbf{v}}_p$ for the relation vector \mathbf{v}_p is calculated from the embeddings of the drug-gene pairs $(d, g) \in \mathcal{R}_p$, while, similar to Eq. (5), the estimator for \mathbf{v}_p can also be calculated from the embeddings of $d \in \mathcal{D}_p$ and $g \in \mathcal{G}_p$. The following equation gives a naive estimator for \mathbf{v}_p :

$$\hat{\mathbf{v}}_{p,\text{naive}} := \mathbf{E}_{\mathcal{G}_p}\{\mathbf{u}_g\} - \mathbf{E}_{\mathcal{D}_p}\{\mathbf{u}_d\}, \quad (\text{S1})$$

$$\mathbf{E}_{\mathcal{D}_p}\{\mathbf{u}_d\} = \frac{1}{|\mathcal{D}_p|} \sum_{d \in \mathcal{D}_p} \mathbf{u}_d, \quad \mathbf{E}_{\mathcal{G}_p}\{\mathbf{u}_g\} = \frac{1}{|\mathcal{G}_p|} \sum_{g \in \mathcal{G}_p} \mathbf{u}_g. \quad (\text{S2})$$

In Eq. (S2), $\mathbf{E}_{\mathcal{D}_p}\{\cdot\}$ and $\mathbf{E}_{\mathcal{G}_p}\{\cdot\}$ are the means over the set of all drugs \mathcal{D} and the set of all genes \mathcal{G} , respectively. Equation (S1) represents the vector difference between the mean vectors of \mathcal{D}_p and \mathcal{G}_p . However, similar to $\hat{\mathbf{v}}_{\text{naive}}$ in Eq. (5), the definition of $\hat{\mathbf{v}}_{p,\text{naive}}$ in Eq. (S1) includes the embeddings of unrelated genes and drugs. Therefore, in Supplementary Information 2.1.1, we compare $\hat{\mathbf{v}}$ and $\hat{\mathbf{v}}_{\text{naive}}$, as well as $\hat{\mathbf{v}}_p$ and $\hat{\mathbf{v}}_{p,\text{naive}}$.

Note the following in setting P2:

- Since $D_p \subset \mathcal{D}_p$ and $D_p = \pi_{\mathcal{D}_p}(\mathcal{R}_p) = \pi_{\mathcal{D}}(\mathcal{R}_p) \subset \pi_{\mathcal{D}}(\mathcal{R}) = D$, it follows that $D_p \subset \mathcal{D}_p \cap D$. For $d \in \mathcal{D}_p \cap D$, there may be $g \in [d] \setminus [d]_p$. Therefore, in Eq. (13), we consider $d \in \mathcal{D}_p \cap D$ and $g \in [d]$, instead of $(d, g) \in \mathcal{R}_p$.

Fig. S1 shows a specific example to illustrate the differences between settings P1 and P2. For drug-gene pairs with drug-gene relations, setting P1 focuses on drugs and genes categorized in the same pathway, while setting P2 considers those genes as well as genes not categorized in the pathway.

1.2 Analogy tasks for drug-gene pairs by year

1.2.1 Global setting by year

Similar to $\hat{\mathbf{v}}$ in Eq. (7), to measure the performance of the estimator $\hat{\mathbf{v}}^y$ in Eq. (21), we prepare the evaluation of the analogy tasks. For $I \in \{(-\infty, \infty), L_y, U_y\}$, using the projection operations in Eq. (10), we define $D^{y|I} := \pi_{\mathcal{D}^y}(\mathcal{R}^{y|I}) \subset \mathcal{D}^y$ and $G^{y|I} := \pi_{\mathcal{G}^y}(\mathcal{R}^{y|I}) \subset \mathcal{G}^y$. Also we define $D^y := D^{y|(-\infty, \infty)}$ and $G^y := G^{y|(-\infty, \infty)}$.

Similar to Eq. (11), for $I \in \{(-\infty, \infty), L_y, U_y\}$, we define $[d]^{y|I} \subset \mathcal{G}^y$ as the set of genes that have drug-gene relations with a drug $d \in D^{y|I}$, and $[g]^{y|I} \subset \mathcal{D}^y$ as the set of drugs that have drug-gene relations with a gene $g \in G^{y|I}$. These are formally defined as follows:

$$[d]^{y|I} := \{g \mid (d, g) \in \mathcal{R}^{y|I}\} \subset \mathcal{G}^y, \quad [g]^{y|I} := \{d \mid (d, g) \in \mathcal{R}^{y|I}\} \subset \mathcal{D}^y. \quad (\text{S3})$$

In particular, we define $[d]^y := [d]^{y|(-\infty, \infty)}$ and $[g]^y := [g]^{y|(-\infty, \infty)}$. Given the above, we perform the analogy tasks in the following setting.

Setting Y1. For the target genes that have drug-gene relations with a drug d , only genes whose relations appeared after year y are considered correct. In other words, for a query drug $d \in D^{y|U_y}$, the set of answer genes is $[d]^{y|U_y}$. The search space is not the set of all genes \mathcal{G}^y , but the gene set $\mathcal{G}^y \setminus [d]^{y|L_y}$. The predicted gene is $\hat{g}_d = \operatorname{argmax}_{g \in \mathcal{G}^y \setminus [d]^{y|L_y}} \cos(\mathbf{u}_d + \hat{\mathbf{v}}^y, \mathbf{u}_g)$, and if $\hat{g}_d \in [d]^{y|U_y}$, then the prediction is considered correct. We define $\hat{g}_d^{(k)}$ as the k -th predicted gene, based on $\cos(\mathbf{u}_d + \hat{\mathbf{v}}^y, \mathbf{u}_g)$ for $g \in \mathcal{G}^y \setminus [d]^{y|L_y}$. For the top- k accuracy, if $\hat{g}_d^{(k)} \in [d]^{y|U_y}$, then the prediction is considered correct.

Setting Y2. For the target genes that have drug-gene relations with a drug d , these genes are considered correct regardless of whether their relations appeared up to or after year y . In other words, for a query drug $d \in D^y$, the set of answer genes is $[d]^y$, where $[d]^y = [d]^{y|(-\infty, \infty)}$. The search space is the set of all genes \mathcal{G}^y . The predicted gene is $\hat{g}_d = \operatorname{argmax}_{g \in \mathcal{G}^y} \cos(\mathbf{u}_d + \hat{\mathbf{v}}^y, \mathbf{u}_g)$, and if $\hat{g}_d \in [d]^y$, then the prediction is considered correct. We define $\hat{g}_d^{(k)}$ as the k -th predicted gene, based on $\cos(\mathbf{u}_d + \hat{\mathbf{v}}^y, \mathbf{u}_g)$ for $g \in \mathcal{G}^y$. For the top- k accuracy, if $\hat{g}_d^{(k)} \in [d]^y$, then the prediction is considered correct.

Note the following in settings Y1 and Y2:

- In setting Y1, the search space is $\mathcal{G}^y \setminus [d]^{y|L_y}$. This ensures that predicted target genes have the relations that appeared only after year y .

	BCV	Ours
$ \mathcal{P} $	136	129
$\sum_{p \in \mathcal{P}} D_p $	4087	3612
$\sum_{p \in \mathcal{P}} \mathcal{D}_p \cap D $	4091	3614
$\sum_{p \in \mathcal{P}} G_p $	1251	1178
$\sum_{p \in \mathcal{P}} \mathcal{G}_p \cap G $	3463	3186
$E_{p \in \mathcal{P}} \{ E_{d \in D_p} \{ [d]_p \} \}$	1.965	1.990
$E_{p \in \mathcal{P}} \{ E_{g \in G_p} \{ [g]_p \} \}$	5.050	4.847

Table S1. Statistics for settings P1 and P2.

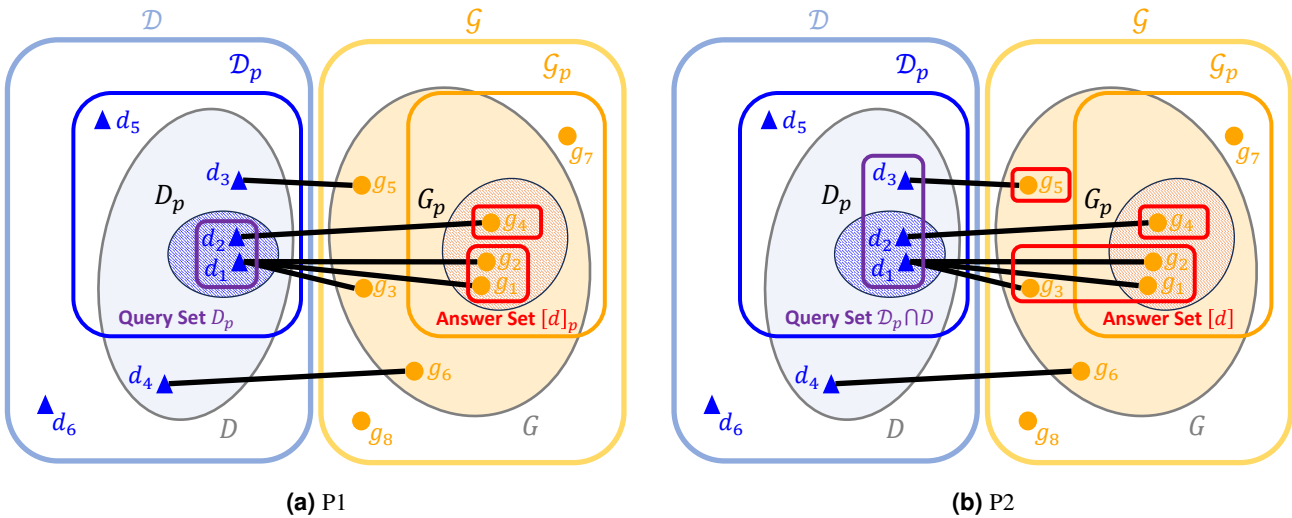


Figure S1. Differences between settings (a) P1 and (b) P2 using a specific example. We set $\mathcal{D} = \{d_1, d_2, d_3, d_4, d_5, d_6\}$, $\mathcal{G} = \{g_1, g_2, g_3, g_4, g_5, g_6, g_7, g_8\}$, and $\mathcal{R} = \{(d_1, g_1), (d_1, g_2), (d_1, g_3), (d_2, g_4), (d_3, g_5), (d_4, g_6)\}$. According to the definitions of D and G , $D = \{d_1, d_2, d_3, d_4\}$ and $G = \{g_1, g_2, g_3, g_4, g_5, g_6\}$. For the pathway p , we set $\mathcal{D}_p = \{d_1, d_2, d_3, d_5\}$ and $\mathcal{G}_p = \{g_1, g_2, g_4, g_7\}$. According to the definition of \mathcal{R}_p , $\mathcal{R}_p = \{(d_1, g_1), (d_1, g_2), (d_2, g_4)\}$. The definitions of D_p and G_p then give $D_p = \{d_1, d_2\}$ and $G_p = \{g_1, g_2, g_4\}$, based on \mathcal{R}_p . In setting P1, the query set is $D_p = \{d_1, d_2\}$, where the set of answer genes for d_1 is $[d_1]_p = \{g_1, g_2\}$ and for d_2 is $[d_2]_p = \{g_4\}$. In setting P2, the query set is $\mathcal{D}_p \cap D = \{d_1, d_2, d_3\}$, where the set of answer genes for d_1 is $[d_1] = \{g_1, g_2, g_3\}$, for d_2 is $[d_2] = \{g_4\}$, and for d_3 is $[d_3] = \{g_5\}$.

- In setting Y2, to evaluate the ability to predict target genes regardless of whether their relations appeared up to or after year y , we consider $(d, g) \in \mathcal{R}^y$ instead of $(d, g) \in \mathcal{R}^{y|U_y}$ in Eq. (20).

1.2.2 Pathway-wise setting by year

Based on the analogy tasks in settings P1, P2, Y1, and Y2, we consider the analogy tasks in the pathway-wise setting by year, where drugs and genes are categorized based on pathways in datasets divided by year.

Consider a fixed year y . When learning embeddings using PubMed abstracts up to year y as training data, we define $\mathcal{D}_p^y \subset \mathcal{D}^y$ and $\mathcal{G}_p^y \subset \mathcal{G}^y$ as the sets of drugs and genes that are categorized in each pathway $p \in \mathcal{P}$ and appeared up to year y , respectively. We then restrict the set \mathcal{R}^y in Eq. (18) to each pathway p and define the subset of the set \mathcal{R}_p^y as follows:

$$\mathcal{R}_p^y := \{(d, g) \in \mathcal{R}^y \mid d \in \mathcal{D}_p^y, g \in \mathcal{G}_p^y\} \subset \mathcal{D}_p^y \times \mathcal{G}_p^y. \quad (\text{S4})$$

For $(d, g) \in \mathcal{R}_p^y$, we divide \mathcal{R}_p^y into two subsets based on whether $y_{(d,g)} \leq y$ or $y < y_{(d,g)}$. Similar to $\mathcal{R}^{y|I}$ in Eq. (19), for an interval I , we define the set $\mathcal{R}_p^{y|I}$, which consists of all $(d, g) \in \mathcal{R}_p^y$ such that $y_{(d,g)} \in I$, as follows:

$$\mathcal{R}_p^{y|I} := \{(d, g) \in \mathcal{R}_p^y \mid y_{(d,g)} \in I\}. \quad (\text{S5})$$

Using $L_y = (-\infty, y]$ and $U_y = (y, \infty)$, the set of drug-gene pairs that satisfies $y_{(d,g)} \leq y$ is $\mathcal{R}_p^{y|L_y}$, and the set of drug-gene pairs that satisfies $y < y_{(d,g)}$ is $\mathcal{R}_p^{y|U_y}$. By definition, $\mathcal{R}_p^{y|L_y} \cap \mathcal{R}_p^{y|U_y} = \emptyset$ and $\mathcal{R}_p^{y|L_y} \cup \mathcal{R}_p^{y|U_y} = \mathcal{R}_p^{y|(-\infty, \infty)} = \mathcal{R}_p^y$.

In analogy tasks, we use “known” $\mathcal{R}_p^{y|L_y}$ and then predict the target genes g from a drug d for (d, g) in “unknown” $\mathcal{R}_p^{y|U_y}$. Using the vector \mathbf{v}_p^y , which represents the drug-gene relations and is derived from $\mathcal{R}_p^{y|L_y}$, we predict \mathbf{u}_g by adding the relation vector \mathbf{v}_p^y to \mathbf{u}_d :

$$\mathbf{u}_d + \mathbf{v}_p^y \approx \mathbf{u}_g. \quad (\text{S6})$$

Similar to equations (13) and (20), Eq. (S6) corresponds to Eq. (4). Therefore, an estimator $\hat{\mathbf{v}}_p^y$ for the relation vector \mathbf{v}_p^y in Eq. (S6) is defined as follows:

$$\hat{\mathbf{v}}_p^y := \mathbb{E}_{\mathcal{R}_p^{y|L_y}} \{ \mathbf{u}_g - \mathbf{u}_d \} = \frac{1}{|\mathcal{R}_p^{y|L_y}|} \sum_{(d,g) \in \mathcal{R}_p^{y|L_y}} (\mathbf{u}_g - \mathbf{u}_d). \quad (\text{S7})$$

where $\mathbb{E}_{\mathcal{R}_p^{y|L_y}} \{ \cdot \}$ is the sample mean over the set of drug-gene pairs $\mathcal{R}_p^{y|L_y}$. Similar to Eq. (7), Eq. (S7) defines the estimator $\hat{\mathbf{v}}_p^y$ as the mean of the vector differences $\mathbf{u}_g - \mathbf{u}_d$ for $(d, g) \in \mathcal{R}_p^{y|L_y}$. For easy comparison with Eq. (5), Eq. (S7) is rewritten as the difference of mean vectors:

$$\hat{\mathbf{v}}_p^y = \mathbb{E}_{\mathcal{R}_p^{y|L_y}} \{ \mathbf{u}_g \} - \mathbb{E}_{\mathcal{R}_p^{y|L_y}} \{ \mathbf{u}_d \}, \quad (\text{S8})$$

$$\mathbb{E}_{\mathcal{R}_p^{y|L_y}} \{ \mathbf{u}_g \} = \frac{1}{|\mathcal{R}_p^{y|L_y}|} \sum_{(d,g) \in \mathcal{R}_p^{y|L_y}} \mathbf{u}_g, \quad \mathbb{E}_{\mathcal{R}_p^{y|L_y}} \{ \mathbf{u}_d \} = \frac{1}{|\mathcal{R}_p^{y|L_y}|} \sum_{(d,g) \in \mathcal{R}_p^{y|L_y}} \mathbf{u}_d. \quad (\text{S9})$$

Similar to $\hat{\mathbf{v}}$ in Eq. (7), to measure the performance of the estimator $\hat{\mathbf{v}}_p^y$ in Eq. (S7), we prepare the evaluation of the analogy tasks. For $I \in \{(-\infty, \infty), L_y, U_y\}$, using the projection operations in Eq. (10), we define $D_p^{y|I} := \pi_{\mathcal{D}_p^y}(\mathcal{R}_p^{y|I})$ and $G_p^{y|I} := \pi_{\mathcal{G}_p^y}(\mathcal{R}_p^{y|I})$. Also we define $D_p^y := D_p^{y|(-\infty, \infty)}$ and $G_p^y := G_p^{y|(-\infty, \infty)}$.

Similar to Eq. (11), for $I \in \{(-\infty, \infty), L_y, U_y\}$, we define $[d]_p^{y|I} \subset \mathcal{G}_p^y$ as the set of genes that have drug-gene relations with a drug $d \in D_p^{y|I}$, and $[g]_p^{y|I} \subset \mathcal{D}_p^y$ as the set of drugs that have drug-gene relations with a gene $g \in G_p^{y|I}$. These are formally defined as follows:

$$[d]_p^{y|I} := \{g \mid (d, g) \in \mathcal{R}_p^{y|I}\} \subset \mathcal{G}_p^y, \quad [g]_p^{y|I} := \{d \mid (d, g) \in \mathcal{R}_p^{y|I}\} \subset \mathcal{D}_p^y. \quad (\text{S10})$$

In particular, we define $[d]_p^y := [d]_p^{y|(-\infty, \infty)}$ and $[g]_p^y := [g]_p^{y|(-\infty, \infty)}$. Similar to settings P1, P2, Y1, and Y2, we perform the analogy tasks in the following four settings.

Setting P1Y1. For the target genes that have drug-gene relations with a drug d , only genes that are categorized in the same pathway p as d and whose relations appeared after year y are considered correct. In other words, for a query drug $d \in D_p^{y|U_y}$, the set of answer genes is $[d]_p^{y|U_y}$. The search space is not the set of all genes \mathcal{G}^y , but the gene set $\mathcal{G}^y \setminus [d]_p^{y|L_y}$. The predicted gene is $\hat{g}_d = \operatorname{argmax}_{g \in \mathcal{G}^y \setminus [d]_p^{y|L_y}} \cos(\mathbf{u}_d + \hat{\mathbf{v}}_p^y, \mathbf{u}_g)$, and if $\hat{g}_d \in [d]_p^{y|U_y}$, then the prediction is considered correct. We define $\hat{g}_d^{(k)}$ as the k -th predicted gene, based on $\cos(\mathbf{u}_d + \hat{\mathbf{v}}_p^y, \mathbf{u}_g)$ for $g \in \mathcal{G}^y \setminus [d]_p^{y|L_y}$. For the top- k accuracy, if $\hat{g}_d^{(k)} \in [d]_p^{y|U_y}$, then the prediction is considered correct.

Setting P2Y1. For the target genes that have drug-gene relations with a drug d , only genes whose relations appeared after year y are considered correct, regardless of whether they are categorized in the same pathway p as the drug d or not. In other words, for a query drug $d \in \mathcal{D}_p^y \cap D^{y|U_y}$, the set of answer genes is $[d]_p^{y|U_y}$. The search space is not the set of all genes \mathcal{G}^y , but the gene set $\mathcal{G}^y \setminus [d]_p^{y|L_y}$. The predicted gene is $\hat{g}_d = \operatorname{argmax}_{g \in \mathcal{G}^y \setminus [d]_p^{y|L_y}} \cos(\mathbf{u}_d + \hat{\mathbf{v}}_p^y, \mathbf{u}_g)$, and if $\hat{g}_d \in [d]_p^{y|U_y}$, then the prediction is considered correct. We define $\hat{g}_d^{(k)}$ as the k -th predicted gene, based on $\cos(\mathbf{u}_d + \hat{\mathbf{v}}_p^y, \mathbf{u}_g)$ for $g \in \mathcal{G}^y \setminus [d]_p^{y|L_y}$. For the top- k accuracy, if $\hat{g}_d^{(k)} \in [d]_p^{y|U_y}$, then the prediction is considered correct.

Setting P1Y2. For the target genes that have drug-gene relations with a drug d , only genes categorized in the same pathway as the drug d are considered correct, regardless of whether their relations appeared up to or after year y . In other words, for a query drug $d \in D_p^y$, the set of answer genes is $[d]_p^y$. The search space is the set of all genes \mathcal{G}^y . The predicted gene

Setting	Query	Answer Set	Search Space
G	$d \in D$	$[d]$	\mathcal{G}
P1	$d \in D_p$	$[d]_p$	\mathcal{G}
P2	$d \in \mathcal{D}_p \cap D$	$[d]$	\mathcal{G}
Y1	$d \in D^{y U_y}$	$[d]^{y U_y}$	$\mathcal{G}^y \setminus [d]^{y L_y}$
Y2	$d \in D^y$	$[d]^y$	\mathcal{G}^y
P1Y1	$d \in D_p^{y U_y}$	$[d]_p^{y U_y}$	$\mathcal{G}^y \setminus [d]_p^{y L_y}$
P2Y1	$d \in \mathcal{D}_p^y \cap D^{y U_y}$	$[d]^{y U_y}$	$\mathcal{G}^y \setminus [d]^{y L_y}$
P1Y2	$d \in D_p^y$	$[d]_p^y$	\mathcal{G}^y
P2Y2	$d \in \mathcal{D}_p^y \cap D^y$	$[d]^y$	\mathcal{G}^y

Table S2. Query, answer set, and search space for each setting for predicting genes from drugs.

is $\hat{g}_d = \operatorname{argmax}_{g \in \mathcal{G}^y} \cos(\mathbf{u}_d + \hat{\mathbf{v}}_p^y, \mathbf{u}_g)$, and if $\hat{g}_d \in [d]_p^y$, then the prediction is considered correct. We define $\hat{g}_d^{(k)}$ as the k -th predicted gene, based on $\cos(\mathbf{u}_d + \hat{\mathbf{v}}_p^y, \mathbf{u}_g)$ for $g \in \mathcal{G}^y$. For the top- k accuracy, if $\hat{g}_d^{(k)} \in [d]_p^y$, then the prediction is considered correct.

Setting P2Y2. For the target genes that have drug-gene relations with a drug d , these genes are considered correct regardless of whether they are categorized in the same pathway or not and whether their relations appeared up to or after year y . In other words, for a query drug $d \in \mathcal{D}_p^y \cap D^y$, the set of answer genes is $[d]^y$. The search space is the set of all genes \mathcal{G}^y . The predicted gene is $\hat{g}_d = \operatorname{argmax}_{g \in \mathcal{G}^y} \cos(\mathbf{u}_d + \hat{\mathbf{v}}_p^y, \mathbf{u}_g)$, and if $\hat{g}_d \in [d]^y$, then the prediction is considered correct. We define $\hat{g}_d^{(k)}$ as the k -th predicted gene, based on $\cos(\mathbf{u}_d + \hat{\mathbf{v}}_p^y, \mathbf{u}_g)$ for $g \in \mathcal{G}^y$. For the top- k accuracy, if $\hat{g}_d^{(k)} \in [d]^y$, then the prediction is considered correct.

Note the following in settings P1Y1, P1Y2, P2Y1 and P2Y2:

- In setting P1Y1, the search space is $\mathcal{G}^y \setminus [d]_p^{y|L_y}$. This ensures that predicted target genes, which are categorized in the same pathway p as the drug d , have the relations that appeared only after year y .
- In setting P2Y1, since $D_p^{y|U_y} \subset \mathcal{D}_p^y$ and $D_p^{y|U_y} = \pi_{\mathcal{D}_p^y}(\mathcal{R}_p^{y|U_y}) = \pi_{\mathcal{D}^y}(\mathcal{R}_p^{y|U_y}) \subset \pi_{\mathcal{D}^y}(\mathcal{R}^{y|U_y}) = D^{y|U_y}$, it follows that $D_p^{y|U_y} \subset \mathcal{D}_p^y \cap D^{y|U_y}$. For $d \in \mathcal{D}_p^y \cap D^{y|U_y}$, there may be $g \in [d]^{y|U_y} \setminus [d]_p^{y|U_y}$. Therefore, in Eq. (S6), we consider $d \in \mathcal{D}_p^y \cap D^{y|U_y}$ and $g \in [d]^{y|U_y}$, instead of $(d, g) \in \mathcal{R}_p^{y|U_y}$. The search space is $\mathcal{G}^y \setminus [d]^{y|L_y}$. This ensure that predicted target genes have the relations that appeared only after year y .
- In setting P1Y2, for a query drug $d \in D_p^y$, to evaluate the ability to predict target genes categorized in the same pathway p as the drug d , regardless of whether their relations appeared up to or after year y , we consider $(d, g) \in \mathcal{R}_p^y$ instead of $(d, g) \in \mathcal{R}_p^{y|U_y}$ in Eq. (20).
- In setting P2Y2, since $D_p^y \subset \mathcal{D}_p^y$ and $D_p^y = \pi_{\mathcal{D}_p^y}(\mathcal{R}_p^y) = \pi_{\mathcal{D}^y}(\mathcal{R}_p^y) \subset \pi_{\mathcal{D}^y}(\mathcal{R}^y) = D^y$, it follows that $D_p^y \subset \mathcal{D}_p^y \cap D^y$. For $d \in \mathcal{D}_p^y \cap D^y$, there may be $g \in [d]^y \setminus [d]_p^y$. Therefore, in Eq. (S6), we consider $d \in \mathcal{D}_p^y \cap D^y$ and $g \in [d]^y$, instead of $(d, g) \in \mathcal{R}_p^{y|U_y}$.

1.3 Comparison of Experimental Settings

Table S2 shows the settings for predicting genes from drugs, as used in the main text. Similarly, Table S3 shows the settings for predicting drugs from genes. In Table S3, we adapted the notations used for predicting genes from drugs in Table S2 to those used for predicting drugs from genes, denoting them as G', P1', P2', Y1', and Y2'.

1.4 Embeddings

The hyperparameters used to train our skip-gram are shown in Table S4.

1.5 Datasets

In the BioConceptVec vocabulary, genes are represented by gene IDs⁵⁴ and drugs are represented by MeSH (Medical Subject Headings, <https://www.nlm.nih.gov/mesh/meshhome.html>) IDs. Therefore, a conversion from IDs to names

Setting	Query	Answer Set	Search Space
G'	$g \in G$	$[g]$	\mathcal{D}
$P1'$	$g \in G_p$	$[g]_p$	\mathcal{D}
$P2'$	$g \in \mathcal{G}_p \cap G$	$[g]$	\mathcal{D}
$Y1'$	$g \in G^{y U_y}$	$[g]^{y U_y}$	$\mathcal{D}^y \setminus [g]^{y L_y}$
$Y2'$	$g \in G^y$	$[g]^y$	\mathcal{D}^y

Table S3. Query, answer set, and search space for each setting for predicting drugs from genes.

Hyperparameter	Values
Training epochs	10
Down-sampling threshold	10^{-5}
Learning rate	0.025
Window size	5
Negative samples	5
Minimal word occurrence	30
Dimension	300

Table S4. Hyperparameter for our skip-gram.

is necessary when performing experiments. In addition, in the data obtained from AsuratDB and the KEGG API, genes are represented by gene IDs and drugs are represented by KEGG IDs. Therefore, a conversion from KEGG IDs to MeSH IDs is also required for use with BioConceptVec. The procedures for converting these IDs are described in the following sections.

1.5.1 Conversion from MeSH ID to drug name

The BioConceptVec vocabulary registers drugs using MeSH (Medical Subject Headings, <https://www.nlm.nih.gov/mesh/meshhome.html>) IDs. This is due to the normalization of drug names using MeSH IDs in PubTator. Therefore, we explain the procedure for converting MeSH IDs to drug names. We used MeSH SPARQL (<https://hhs.github.io/meshrdf/sparql-and-uri-requests>) to obtain the MeSH headings corresponding to the MeSH IDs in the BioConceptVec vocabulary. We used these headings to convert MeSH IDs to drug names. We also applied this conversion to drugs in the vocabulary of our trained skip-gram model.

1.5.2 Conversion from gene ID to gene name

The BioConceptVec vocabulary registers genes using gene IDs. Therefore, we explain the procedure for converting gene IDs to gene names. We used the KEGG API to obtain the names corresponding to the gene IDs in the BioConceptVec vocabulary. This API allows for batch requests; for example, to process gene IDs 20, 21, 22, 23, 24, the data is available at <https://rest.kegg.jp/list/hsa:20+hsa:21+hsa:22+hsa:23+hsa:24>. If multiple names corresponded to a single gene ID, we chose the first name. We also applied this conversion to genes in the vocabulary of our trained skip-gram model.

1.5.3 Conversion from KEGG ID to MeSH ID

In AsuratDB and the KEGG API, which is used to obtain drug-gene relations, genes are represented by gene IDs, while drugs are represented by KEGG IDs. Therefore, to use the data in BioConceptVec, we need to convert the KEGG IDs to MeSH IDs. We followed a four-step procedure (I), (II), (III), and (IV) to convert KEGG IDs to MeSH IDs.

(I) KEGG ID to PubChem SID or ChEBI ID Some drugs in KEGG are manually linked to external databases such as PubChem (<https://pubchem.ncbi.nlm.nih.gov/>) and ChEBI (<https://www.ebi.ac.uk/chebi/>), which are larger databases than KEGG. Therefore, we used these databases to link their IDs to MeSH IDs.

Since PubChem is maintained by the NCBI (National Center for Biotechnology Information, <https://www.ncbi.nlm.nih.gov/>) that also maintains the MeSH database, we prioritized the conversion of KEGG IDs to PubChem Substance IDs (SIDs). If we could not convert KEGG IDs directly to PubChem SIDs, we converted them to ChEBI IDs. The conversion from KEGG IDs to PubChem SIDs is available at <https://rest.kegg.jp/conv/pubchem/drug>, and the conversion to ChEBI IDs is available at <https://rest.kegg.jp/conv/chebi/drug>.

Embeddings	Setting	Method	Centering	Top1	Top10	MRR
G		Random		0.000	0.000	0.001
		\hat{v}_{naive}		0.067	0.197	0.111
		\hat{v}	✓	0.125	0.381	0.209
		\hat{v}	✓	0.206	0.455	0.289
Ours	P1	Random		0.000	0.001	0.001
		$\hat{v}_{p,\text{naive}}$		0.364	0.661	0.470
		\hat{v}_p	✓	0.455	0.810	0.581
		\hat{v}_p	✓	0.589	0.862	0.685
Ours	P2	Random		0.000	0.001	0.001
		$\hat{v}_{p,\text{naive}}$		0.376	0.682	0.484
		\hat{v}_p	✓	0.473	0.837	0.601
		\hat{v}_p	✓	0.530	0.803	0.626
		\hat{v}_p	✓	0.600	0.880	0.700

Table S5. Results of the naive estimators and the centering ablation study for settings G, P1, and P2.

(II) PubChem SID or ChEBI ID to PubChem CID Next, we converted PubChem SIDs and ChEBI IDs to PubChem Compound IDs (CIDs), which are associated with MeSH IDs. The conversion from PubChem SIDs to PubChem CIDs is available at <https://pubchem.ncbi.nlm.nih.gov/rest/pug/substance/sourceall/KEGG/cids/json>. To convert ChEBI IDs to PubChem CIDs, we used the PubChem API. For example, for ChEBI ID 39112, the corresponding data can be obtained at <https://pubchem.ncbi.nlm.nih.gov/rest/pug/compound/xref/RegistryID/chebi:39112/cids/json>.

(III) Convert CIDs to MeSH Headings We used the Entrez (<https://www.ncbi.nlm.nih.gov/Web/Search/entrezfs.html>) System API provided by NCBI, and obtained the MeSH headings associated with each CID. This API allows for batch requests. For example, for CIDs 5328940 and 156413, the corresponding data can be obtained at <https://eutils.ncbi.nlm.nih.gov/entrez/eutils/esummary.fcgi?db=pccompound&id=5328940,156413&retmode=json>.

(IV) MeSH Headings to MeSH ID Since we had already obtained the correspondence between MeSH IDs and MeSH headings in Supplementary Information 1.5.1, we could match MeSH IDs with the MeSH headings obtained through the Entrez system API. In this way, we converted the original KEGG IDs to MeSH IDs. Note that multiple KEGG IDs may correspond to the same MeSH ID. In such cases, we chose the smallest KEGG ID to associate with the MeSH ID.

2 Details of experimental results

2.1 Analogy tasks for drug-gene pairs

2.1.1 Comparison of estimators and centering ablation study

For settings G, P1, and P2, Table S5 shows the results of the naive estimators defined in equations (5) and (S1) and the centering ablation study, using our skip-gram. In all settings, the results of the estimators \hat{v} and \hat{v}_p calculated from drug-gene relations outperformed those of the naive estimators \hat{v}_{naive} and $\hat{v}_{p,\text{naive}}$. We also observed performance improvements due to centering. Based on this, we showed the results using the estimators calculated from the drug-gene relations with centering applied in Table 3.

2.1.2 Prediction of drugs from genes

As seen in Supplementary Information 1.3, Table S3 defines settings G' , $P1'$, and $P2'$ for the analogy tasks for predicting drugs from genes. We then define estimators to perform the analogy tasks in these settings. Similar to the estimator \hat{v} in Eq. (7) for

Embed.	Setting	Method	Metric		
			Top1	Top10	MRR
BCV	G'	Random	0.000	0.001	0.001
		$\hat{\mathbf{v}}'$	0.233	0.560	0.345
	P1'	Random	0.000	0.001	0.001
		$\hat{\mathbf{v}}'_p$	0.426	0.679	0.515
	P2'	Random	0.000	0.001	0.001
		$\hat{\mathbf{v}}'_p$	0.248	0.507	0.337
Ours	G'	Random	0.000	0.003	0.002
		$\hat{\mathbf{v}}'$	0.240	0.577	0.351
	P1'	Random	0.000	0.003	0.002
		$\hat{\mathbf{v}}'_p$	0.478	0.751	0.571
	P2'	Random	0.000	0.003	0.002
		$\hat{\mathbf{v}}'_p$	0.279	0.516	0.359

Table S6. Gene prediction performance in settings G', P1', and P2'.

	1970	1975	1980	1985	1990	1995	2000	2005	2010	2015	2020
$ \mathcal{D}^y $	2268	3275	5059	7125	9387	11748	14044	16827	19758	22717	25431
$ \mathcal{G}^y $	353	725	1782	3413	5976	10533	16949	24784	32264	39961	47509
$ \mathcal{R}^y ^{L_y}$	12	37	117	256	499	859	1269	1637	1978	2354	2603
$ \mathcal{R}^y ^{U_y}$	13	53	183	296	344	515	473	379	281	189	61
$ D^y ^{U_y} $	12	48	154	272	288	369	325	256	189	131	48
$ D^y $	22	79	246	475	663	893	1047	1151	1269	1423	1495
$ G^y ^{U_y} $	6	14	34	55	89	137	173	153	140	115	44
$ G^y $	8	20	46	74	122	215	325	398	477	540	570
$E_{d \in D^y L_y} \{ [d]^y ^{L_y} \}$	1.091	1.028	1.104	1.133	1.188	1.372	1.500	1.613	1.665	1.722	1.760
$E_{d \in D^y U_y} \{ [d]^y ^{U_y} \}$	1.083	1.104	1.188	1.088	1.194	1.396	1.455	1.480	1.487	1.443	1.271
$E_{g \in G^y L_y} \{ [g]^y ^{L_y} \}$	3.000	2.467	4.179	5.020	5.940	5.335	4.789	4.547	4.425	4.467	4.591
$E_{g \in G^y U_y} \{ [g]^y ^{U_y} \}$	2.167	3.786	5.382	5.382	3.865	3.759	2.734	2.477	2.007	1.643	1.386

Table S7. Statistics for settings Y1 and Y2.

setting G, we define the estimator $\hat{\mathbf{v}}'$ for setting G':

$$\hat{\mathbf{v}}' := -\hat{\mathbf{v}} = E_{\mathcal{R}} \{ \mathbf{u}_d - \mathbf{u}_g \} = \frac{1}{|\mathcal{R}|} \sum_{(d,g) \in \mathcal{R}} (\mathbf{u}_d - \mathbf{u}_g). \quad (\text{S11})$$

Similar to the estimator $\hat{\mathbf{v}}_p$ in Eq. (14) for settings P1 and P2, we also define the estimator $\hat{\mathbf{v}}'_p$ for settings P1' and P2':

$$\hat{\mathbf{v}}'_p := -\hat{\mathbf{v}}_p = E_{\mathcal{R}_p} \{ \mathbf{u}_d - \mathbf{u}_g \} = \frac{1}{|\mathcal{R}_p|} \sum_{(d,g) \in \mathcal{R}_p} (\mathbf{u}_d - \mathbf{u}_g). \quad (\text{S12})$$

For settings G', P1', and P2', we performed the analogy tasks using $\hat{\mathbf{v}}'$ and $\hat{\mathbf{v}}'_p$, and Table S6 shows the results. Similar to Table 3, the estimators calculated from the drug-gene relations outperformed the random baseline.

While Table 3 shows higher scores for setting P2 compared to setting P1, Table S6 shows higher scores for setting P1' compared to setting P2'. To explain these results, we focus on the sizes of the query and answer sets, using actual values from BioConceptVec. As shown in Table S1, the sizes of the query sets for settings P1 and P2 are $\sum_{p \in \mathcal{P}} |D_p| = 4087$ and $\sum_{p \in \mathcal{P}} |\mathcal{D}_p \cap D| = 4091$, respectively. The ratio is $\sum_{p \in \mathcal{P}} |\mathcal{D}_p \cap D| / \sum_{p \in \mathcal{P}} |D_p| \approx 1.001$. On the other hand, for settings

Metric	Setting	Method	Year										
			1970	1975	1980	1985	1990	1995	2000	2005	2010	2015	2020
Top1	Y1	Random	0.000	0.000	0.003	0.000	0.000	0.001	0.000	0.000	0.000	0.000	0.000
		\hat{v}^y	0.250	0.333	0.208	0.165	0.132	0.076	0.092	0.062	0.090	0.107	0.021
	Y2	Random	0.005	0.005	0.000	0.000	0.000	0.000	0.000	0.000	0.000	0.000	0.000
		\hat{v}^y	0.500	0.481	0.350	0.318	0.305	0.299	0.328	0.326	0.318	0.376	0.318
Top10	Y1	Random	0.008	0.010	0.008	0.002	0.003	0.001	0.000	0.001	0.001	0.000	0.000
		\hat{v}^y	0.500	0.625	0.487	0.438	0.410	0.347	0.397	0.352	0.344	0.328	0.271
	Y2	Random	0.041	0.022	0.007	0.003	0.002	0.001	0.001	0.001	0.000	0.000	0.000
		\hat{v}^y	0.727	0.785	0.699	0.657	0.665	0.679	0.735	0.744	0.702	0.773	0.764
MRR	Y1	Random	0.012	0.007	0.005	0.003	0.002	0.002	0.001	0.001	0.000	0.000	0.000
		\hat{v}^y	0.331	0.438	0.304	0.253	0.214	0.163	0.182	0.147	0.173	0.188	0.103
	Y2	Random	0.017	0.010	0.006	0.003	0.002	0.002	0.001	0.001	0.001	0.000	0.000
		\hat{v}^y	0.590	0.592	0.476	0.434	0.425	0.429	0.468	0.463	0.451	0.513	0.469

Table S8. Gene prediction performance in settings Y1 and Y2.

	1970	1975	1980	1985	1990	1995	2000	2005	2010	2015	2020
$\sum_{p \in \mathcal{P}} D_p^{y U_y} $	14	104	314	507	521	601	526	439	312	201	67
$\sum_{p \in \mathcal{P}} \mathcal{D}_p^y \cap D^{y U_y} $	16	115	363	572	573	732	644	529	401	264	98
$\sum_{p \in \mathcal{P}} \mathcal{D}_p^y $	26	156	513	959	1363	1728	1999	2205	2419	2711	2821
$\sum_{p \in \mathcal{P}} \mathcal{D}_p^y \cap D^y $	30	174	566	1028	1419	1794	2068	2263	2480	2773	2886
$\sum_{p \in \mathcal{P}} G_p^{y U_y} $	6	29	88	129	195	305	326	269	228	168	62
$\sum_{p \in \mathcal{P}} \mathcal{G}_p^y \cap G^{y U_y} $	15	50	177	281	520	935	1087	859	774	682	275
$\sum_{p \in \mathcal{P}} \mathcal{G}_p^y $	6	38	110	170	281	484	658	772	925	1066	1124
$\sum_{p \in \mathcal{P}} \mathcal{G}_p^y \cap G^y $	18	68	207	367	652	1356	2015	2359	3087	3518	3627
$E_{p \in \mathcal{P}} \left\{ E_{d \in D_p} \left\{ [d]_p^{y L_y} \right\} \right\}$	4.000	2.500	5.921	8.148	11.407	12.667	14.319	14.649	14.631	15.465	15.977
$E_{p \in \mathcal{P}} \left\{ E_{d \in D_p} \left\{ [d]_p^{y U_y} \right\} \right\}$	2.333	4.160	6.038	7.243	6.432	7.805	6.188	5.776	5.032	4.467	3.190
$E_{p \in \mathcal{P}} \left\{ E_{g \in G_p} \left\{ [g]_p^{y L_y} \right\} \right\}$	1.000	1.136	1.789	1.918	2.444	3.441	4.483	5.216	5.529	6.171	6.400
$E_{p \in \mathcal{P}} \left\{ E_{g \in G_p} \left\{ [g]_p^{y U_y} \right\} \right\}$	1.000	1.160	1.692	1.843	2.407	3.961	3.835	3.539	3.677	3.733	2.952

Table S9. Statistics for settings P1Y1, P1Y2, P2Y1, and P2Y2.

P1' and P2', the sizes of the query sets are $\sum_{p \in \mathcal{P}} |G_p| = 1251$ and $\sum_{p \in \mathcal{P}} |\mathcal{G}_p \cap G| = 3463$, respectively, with a ratio of $\sum_{p \in \mathcal{P}} |\mathcal{G}_p \cap G| / \sum_{p \in \mathcal{P}} |G_p| \approx 2.768$. For settings P1, P2, P1', and P2', the answer sets defined in Tables S2 and S3 are $[d]_p$, $[d]$, and $[g]_p$, $[g]$, respectively. By definition, the sizes of the answer sets satisfy $|[d]_p| \leq |[d]|$ and $|[g]_p| \leq |[g]|$. In fact, the expected values of them are $E_{p \in \mathcal{P}} \{E_{d \in D_p} \{|[d]_p|\}\} = 1.965$, $E_{d \in D} \{|[d]| \} = 2.938$, $E_{p \in \mathcal{P}} \{E_{g \in G_p} \{|[g]_p|\}\} = 5.050$, and $E_{g \in G} \{|[g]|\} = 10.008$, respectively. In settings P1 and P2, the sizes of the query sets are nearly identical, but the larger answer sets in setting P2 probably make the task easier. On the other hand, the sizes of the query sets in setting P2' are more than twice as large as those in P1', which likely contributes to the lower evaluation metric scores in setting P2'.

2.2 Analogy tasks for drug-gene pairs by year

2.2.1 Global setting by year

Table S7 shows the statistics for settings Y1 and Y2. As seen in Table S2, in setting Y1, the query is $d \in D^{y|U_y}$, and the search space is $\mathcal{G}^y \setminus [d]^{y|L_y}$. In setting Y2, the query is $d \in D^y$, and the search space is \mathcal{G}^y . Table S7 shows that $D^{y|U_y}$ has increased since 1970 and started to decrease after 1995. On the other hand, D^y and \mathcal{G}^y show a monotonic increase over the years.

We showed the plots of the results for settings Y1 and Y2 in Fig. 3. For settings Y1 and Y2, Table S8 shows detailed results used in Fig. 3.

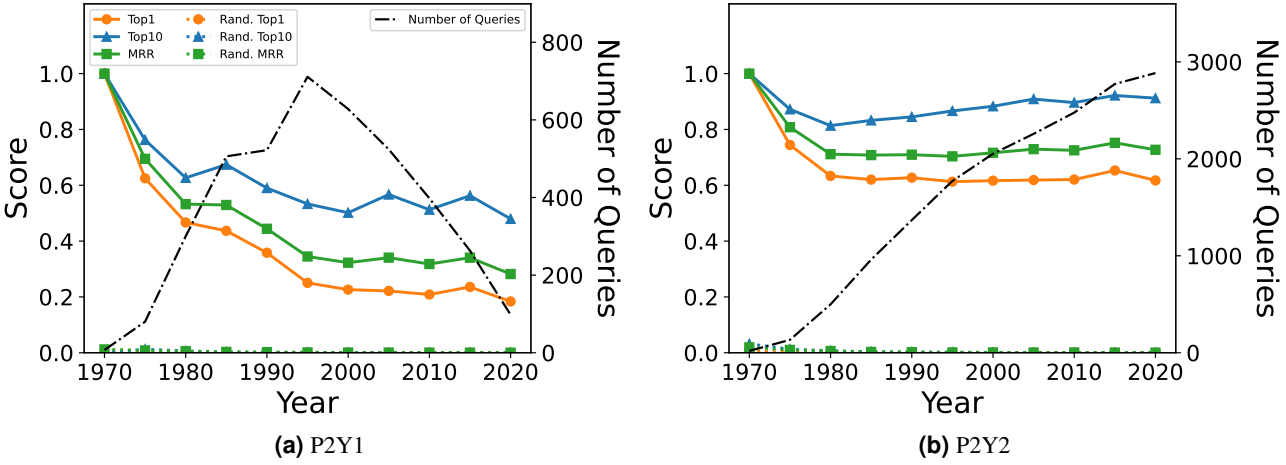


Figure S2. Gene prediction performance and the number of queries for each year in settings P2Y1 and P2Y2.

2.2.2 Pathway-wise setting by year

Table S9 shows the statistics for settings P1Y1, P1Y2, P2Y1, and P2Y2. As seen in Table S2, the query is $d \in D_p^{y|U_y}$ in setting P1Y1, $d \in D_p^y$ in setting P1Y2, $d \in D_p^y \cap D^{y|U_y}$ in P2Y1, and $d \in D_p^y \cap D^y$ in setting P2Y2. Table S9 shows that $D_p^{y|U_y}$ and $D_p^y \cap D^{y|U_y}$ have increased since 1970 and started to decrease after 1995. On the other hand, D_p^y and $D_p^y \cap D^y$ show a monotonic increase over the years.

We showed the plots of the results for settings P1Y1 and P1Y2 in Fig. 3. Fig. S2 shows the plots of the results for settings P2Y1 and P2Y2. For settings P1Y1, P1Y2, P2Y1, and P2Y2, Table S10 shows detailed results used in Fig. 3 and Fig. S2. As shown in Table 3, settings P1 and P2 show roughly the same trends. Similarly, in Table S10, settings P1Y1 and P2Y1, as well as P1Y2 and P2Y2, each show similar trends.

Metric	Setting	Method	Year										
			1970	1975	1980	1985	1990	1995	2000	2005	2010	2015	2020
Top1	P1Y1	Random	0.014	0.000	0.001	0.001	0.000	0.000	0.000	0.000	0.000	0.000	0.000
		\hat{v}_p^y	1.000	0.653	0.515	0.484	0.394	0.303	0.275	0.263	0.256	0.285	0.269
	P1Y2	Random	0.000	0.001	0.001	0.000	0.000	0.000	0.000	0.000	0.000	0.000	0.000
		\hat{v}_p^y	1.000	0.780	0.674	0.656	0.651	0.633	0.636	0.627	0.630	0.659	0.623
	P2Y1	Random	0.000	0.000	0.000	0.000	0.000	0.000	0.000	0.000	0.000	0.000	0.000
		\hat{v}_p^y	1.000	0.625	0.467	0.437	0.358	0.250	0.226	0.221	0.209	0.236	0.184
	P2Y2	Random	0.005	0.003	0.001	0.000	0.000	0.000	0.000	0.000	0.000	0.000	0.000
		\hat{v}_p^y	1.000	0.744	0.633	0.620	0.627	0.613	0.616	0.619	0.621	0.653	0.617
Top10	P1Y1	Random	0.029	0.020	0.009	0.003	0.003	0.001	0.002	0.001	0.000	0.000	0.000
		\hat{v}_p^y	1.000	0.800	0.670	0.727	0.638	0.597	0.573	0.627	0.566	0.665	0.612
	P1Y2	Random	0.026	0.012	0.005	0.004	0.004	0.002	0.002	0.001	0.001	0.001	0.000
		\hat{v}_p^y	1.000	0.906	0.842	0.863	0.863	0.879	0.896	0.913	0.899	0.925	0.911
	P2Y1	Random	0.000	0.013	0.006	0.002	0.002	0.001	0.001	0.000	0.000	0.000	0.000
		\hat{v}_p^y	1.000	0.762	0.627	0.674	0.590	0.533	0.502	0.567	0.513	0.563	0.480
	P2Y2	Random	0.032	0.013	0.007	0.004	0.002	0.002	0.001	0.001	0.000	0.000	0.001
		\hat{v}_p^y	1.000	0.872	0.814	0.832	0.845	0.866	0.883	0.909	0.896	0.922	0.912
MRR	P1Y1	Random	0.032	0.008	0.005	0.003	0.002	0.001	0.001	0.001	0.001	0.000	0.001
		\hat{v}_p^y	1.000	0.727	0.583	0.582	0.483	0.404	0.378	0.392	0.373	0.410	0.391
	P1Y2	Random	0.023	0.011	0.005	0.003	0.002	0.001	0.001	0.001	0.001	0.000	0.000
		\hat{v}_p^y	1.000	0.843	0.749	0.743	0.731	0.722	0.734	0.737	0.732	0.758	0.731
	P2Y1	Random	0.012	0.008	0.006	0.003	0.002	0.001	0.001	0.001	0.001	0.000	0.000
		\hat{v}_p^y	1.000	0.695	0.532	0.529	0.444	0.345	0.323	0.341	0.318	0.340	0.282
	P2Y2	Random	0.019	0.010	0.006	0.003	0.002	0.001	0.001	0.001	0.001	0.001	0.000
		\hat{v}_p^y	1.000	0.808	0.711	0.708	0.709	0.704	0.716	0.729	0.725	0.752	0.727

Table S10. Gene prediction performance in settings P1Y1, P1Y2, P2Y1, and P2Y2.